# Connection between asymptotic normalization coefficients and resonance widths of mirror states

A. M. Mukhamedzhanov

Phys. Rev. C **99**, 024311 — Published 19 February 2019

DOI: 10.1103/PhysRevC.99.024311

# Connection between asymptotic normalization coefficients and resonance widths of mirror states

A. M. Mukhamedzhanov
*Cyclotron Institute, Texas A&M University, College Station, TX 77843*

Asymptotic normalization coefficients (ANCs) are fundamental nuclear constants playing important role in nuclear reactions, nuclear structure and nuclear astrophysics. In this paper a connection between ANCs and resonance widths of the mirror states is established. Using Pinkston-Satchler equation the ratio for resonance widths and ANCs of mirror nuclei is obtained in terms of the Wronskians from the radial overlap functions and regular solutions of the two-body Schrödinger equation with the short-range interaction excluded. This ratio allows one to use microscopic overlap functions for mirror nuclei in the internal region, where they are the most accurate, to correctly predict the ratio of the resonance widths and ANCs for mirror nuclei, which determine the amplitudes of the tails of the overlap functions. If the microscopic overlap functions are not available one can express the Wronskians for the resonances and mirror bound states in terms of the corresponding mirror two-body potential-model wave functions. A further simplification of the Wronskians ratio leads to the equation for the ratio of the resonance widths and mirror ANCs, which is expressed in terms of the ratio of the two-body Coulomb scattering wave functions at the resonance energy and at the binding energy [N. K. Timofeyuk, R. C. Johnson, and A. M. Mukhamedzhanov, Phys. Rev. Lett. **91**, 232501 (2003]. Calculations of the ratios of resonance widths and mirror ANCs for different nuclei are presented. From this ratio one can determine the resonance width if the mirror ANC is known and vice versa. Comparisons with available experimental ratios are done.

PACS numbers: 21.10.Jx, 21.60.De,25.40.Ny, 24.10.-i

## I. INTRODUCTION

The asymptotic normalization coefficient (ANC) is a fundamental nuclear characteristics of bound states [1, 2] playing an important role in nuclear reaction and structure physics. The ANCs determine the normalization of the peripheral part of transfer reaction amplitudes [1, 2] and overall normalization of the peripheral radiative capture processes [3–6]. In the $R$-matrix approach the ANC determines the normalization of the external nonresonant radiative capture amplitude and the channel radiative reduced width amplitude [7–9]. In [10, 11] relationships between mirror proton and neutron ANCs were obtained.

Pairs of nuclei $B_1$ and $B_2$ are mirror nuclei if the number of protons $Z_1$ of nucleus $B_1$ equals the number of neutrons $N_2$ of $B_2$ and the number of protons of $B_2$ $Z_2$ equals the number of neutrons $N_1$ of $B_1$, such that the mass number of both nuclei is the same ($A = N_1 + Z_1 = N_2 + Z_2$). The experimental data from mirror nuclei show charge symmetry of the nuclear force. It is assumed that charge symmetry rather than full charge independence is involved because mirror nuclei have the same number of $p - n$ pairs.

However, the ANCs are important characteristics not only of the bound states but also resonances, see [9]. The width of a narrow resonance can be expressed in terms of the ANC of the Gamow wave function or of the $R$-matrix resonant outgoing wave. That is why the relationship between the ANCs of mirror bound states [10, 11] can be extended to the relationship between resonance widths and ANCs of the mirror nuclei. The calculated resonance widths and the ANCs themselves depend strongly on the choice of the nucleon-nucleon (NN) force but the ratios of the resonance widths and the ANCs for mirror pairs should not depend on the choice of the NN force. This observation is based thus far entirely on the calculations using detailed models of nuclear structure. It follows naturally as a consequence of the charge symmetry of nuclear forces. Mirror nuclei have the same quantum numbers of mirror states (for more detailed discussion of mirror symmetry see [12]).

Another important for the present paper feature of the mirror nuclei is a similarity of the internal mirror wave functions. Let us consider a mirror pair in two-body potential model, which is used in the present paper: $B_1 = (a_1\, A_1)$ in the resonance state and the loosely bound nucleus $B_2 = (a_2\, A_2)$. The mirror resonance state is obtained by the replacement of one of the neutrons by a proton. The additional Coulomb interaction pushes the bound-state level into a resonance level. The resonance and binding energy of the mirror states are significantly smaller than the depth of the nuclear potential. The Coulomb interaction is almost a constant in the nuclear interior. Hence, in the nuclear interior, which all that matters to determine the ratio of the resonance width and the ANC of the mirror state, the radial behavior of the mirror wave functions is very similar and they differ only by normalization. In the external region the resonant and bound-state wave functions differ.

The first attempt to relate the resonance width and the ANC of the mirror nuclei was done in [10]. In this paper, the relationship between the resonance widths and the ANCs is established based on the Pinkston-Satchler equation

used in [11] for the ANCs of the mirror bound states. The obtained ratio of the resonance width and the ANC of the mirror bound state is expressed in terms of the ratio of the Wronskians containing the overlap functions of the mirror resonance and bound states in the internal region where the radial behavior of the mirror overlap functions is very similar and can be calculated quite accurately using *ab initio* approach. If these overlap functions are not available, as an approximation they can be replaced by the mirror resonance and bound state wave functions calculated using the two-body potential model with the same potentials for the resonance and bound states. Assuming that the radial behavior of the mirror resonant and bound-state wave functions is identical in the nuclear interior one can replace the Wronskian ratio for the resonance width and the ANC of the mirror bound state by the equation derived in [10], which does not require a knowledge of the internal resonant and bound-state wave functions.

Connection between the ANC and the resonance width of the mirror resonance state provides a powerful indirect method to obtain information which is unavailable directly. If, for instance, the resonance width is unknown it can be determined through the known ANC of the mirror state and vice versa. For example, near the edge of the stability valley neutron binding energies become so small, that the mirror proton states are resonances. Using the relationship between the mirror resonance width and the ANC the resonance width can be determined. Also loosely bound states $\alpha + A$ become resonances in the mirror nucleus $\alpha + B$, where charge $Z_B e > Z_A e$. Using the method developed here one can find one of the missing quantities, the resonance width of the narrow resonance state or the mirror ANC. In what follows the system of units in which $\hbar = c = 1$ is used throughout the paper.

## II. ANC AND RESONANCE WIDTH

### A. ANC as residue of $S$ matrix

The ANC enters the theory in two ways [1]. In the scattering theory the residue at the poles of the elastic scattering $S$ matrix corresponding to bound states can be expressed in terms of the ANC:

$$S^{J_B}_{l_B\, j_B; l_B\, j_B} \xrightarrow{k_{aA}\to k^{bs}_{aA}} \frac{A_{l_B\, j_B}}{k - i\,\kappa_{aA}} \tag{1}$$

with the residue

$$A^{J_B}_{l_B\, j_B} = -i^{2\,l_B+1}\, e^{i\,\pi\,\eta^{bs}_{aA}}\, \left(C^{B}_{aA\, l_B\, j_B\, J_B}\right)^2. \tag{2}$$

Here, $C^{B}_{aA\, l_B\, j_B\, J_B}$ is the ANC for the virtual decay of the bound state $B(aA)$ in the channel with the relative orbital angular momentum $l_B$ of $a$ and $A$, the total angular momentum $j_B$ of $a$ and total angular momentum $J_B$ of the system $a + A$, $k_{aA}$ is the relative momentum of particles $a$ and $A$.

$$\eta^{bs}_{aA} = \frac{Z_a\, Z_A\, e^2\, \mu_{aA}}{\kappa_{aA}} \tag{3}$$

is the Coulomb parameter for the bound state $B = (a\,A)$, $\kappa_{aA} = \sqrt{2\,\mu_{aA}\,\varepsilon_{aA}}$ is the bound-state wave number, $\varepsilon_B = m_a + m_A - m_B$ is the binding energy for the virtual decay $B \to a + A$, $Z_i\, e$ and $m_i$ is the charge and mass of particle $i$, and $\mu_{aA}$ is the reduced mass of $a$ and $A$. Note that the singling out the factor $e^{i\,\pi\,\eta^{bs}_{aA}}$ in the residue makes the ANC for bound states real.

Equations (1) and (2), which were proved for the bound states in [13–18], can be extended for resonance states.

### B. Connection between ANC and resonance width

The proof of the connection between the residue in the resonance pole of the elastic scattering $S$ matrix and the ANC of the resonance state is not trivial. In this section is presented a general proof of the connection of the residue in the pole of the $S_{l_B}(k_{aA})$ matrix element with the ANC , which is valid both for the bound states and resonances. The potential is given by the sum of the short-range nuclear plus the long-range Coulomb potentials. Taking into account that the residue of the elastic scattering $S$ matrix in the resonance pole is expressed in terms of the resonance width, one can obtain a connection between the ANC and the resonance width.

Let me consider two spinless particles $a$ and $A$ with relative momentum $k^2_{aA} = 2\,\mu_{aA}\,E_{aA}$, relative energy $E_{aA}$ and the reduced mass $\mu_{aA}$ in the partial wave $l_B$ at which the system $B = a + A$ has a resonance or a bound state. The

radial wave function $\psi_{k_{aA}l_B}(r) = \frac{u_{k_{aA}l_B}(r)}{r}$ satisfies the Schrödinger equation in the partial wave $l_B$:

$$\frac{\partial^2 u_{k_{aA}l_B}(r)}{\partial r^2} + \big[k_{aA}^2 - 2\mu_{aA}V(r) \; - \; \frac{l_B(l_B+1)}{r^2}\big] u_{k_{aA}l_B}(r) = 0. \tag{4}$$

Here $V(r) = V^N(r) + V^C(r)$, $V^N(r)$ is the short-range nuclear potential and $V^C(r)$ is the long-range Coulomb one. For potentials satisfying the condition $\lim\limits_{r\to 0} r^2\, V(r) \to 0$

$$u_{k_{aA}l_B}(r) \sim r^{l_B+1}, \qquad r \to 0. \tag{5}$$

Now one should take the derivative over $k_{aA}$ from the left-hand-side of Eq. (4), multiply the result by $u_{k_{aA}l_B}(r)$ and subtract from it Eq. (4) multiplied by $\partial u_{k_{aA}l_B}(r)/\partial k_{aA}$. Integrating the obtained expression from $r = 0$ until $r = R$ and taking into account Eq. (5) one gets

$$\int\limits_0^R dr\, u^2_{k_{aA}l_B}(r) = \frac{1}{2k_{aA}} \left[\frac{\partial u_{k_{aA}l_B}(R)}{\partial k_{aA}} \frac{\partial u_{k_{aA}l_B}(R)}{\partial R} - u_{k_{aA}l_B}(R) \frac{\partial^2 u_{k_{aA}l_B}(R)}{\partial k_{aA}\, \partial R}\right]. \tag{6}$$

Taking $R$ so large that $u_{k_{aA}l_B}(R)$ can be replaced by its leading asymptotic term one gets the elastic scattering wave function

$$u_{k_{aA}l_B}(R) \approx \tilde{C}_{l_B} \left[e^{i\rho} - (-1)^{l_B}\, S^{-1}_{l_B}(k_{aA}) e^{-i\rho}\right], \tag{7}$$

where $\rho = k_{aA}R - \eta_{aA}\, \ln 2k_{aA}R$, $\eta_{aA} = \frac{Z_a\, Z_A\, e^2\, \mu_{aA}}{k_{aA}}$ is the Coulomb parameter of the $a + A$ system,

$$S_{l_B}(k_{aA}) = e^{2\,i\,[\sigma^C_{l_B}(k_{aA}) + \delta^{CN}_{l_B}(k_{aA})]} \tag{8}$$

is the elastic scattering $S$-matrix element, $\sigma^C_{l_B}(k_{aA})$ and $\delta^{CN}_{l_B}(k_{aA})$ are the Coulomb and Coulomb-modified nuclear scattering phase shifts in the $l_B$-th partial wave, $\tilde{C}_{l_B}$ is a constant , which is in the pole of the $S$-matrix is related to the corresponding ANC $C_{l_B}$, see Eqs (14) and (15) below. Note that the scattering wave function $u_{k_{aA}l_B}$ at large $R$ at real momentum $k_{aA}$ contains ingoing and outgoing waves and is not normalizable in the entire space.

Assume that the elastic scattering $S_{l_B}(k_{aA})$-matrix element has a first order pole at $k_{aA} = k_p$ with the residue $A_{l_B}$ corresponding to the bound state $k_p = i\,\kappa_{aA}$ or to the resonance $k_p = k_{aA(\mathcal{R})} = k_{aA\,(0)} - \mathrm{Im}k_{aA\,(\mathcal{R})}$, where $k_{aA\,(0)} = \mathrm{Re}k_{aA\,(\mathcal{R})}$:

$$S_{l_B}(k_{aA}) = \frac{A_{l_B}}{k_{aA} - k_p} + g_{l_B}(k_{aA}), \tag{9}$$

where $g_{l_B}(k_{aA})$ is a regular function at $k_{aA} = k_p$.

Substituting Eqs (7) and (9) into the right-hand-side of Eq. (6) and performing the differentiation over $k_{aA}$ and $R$ and taking $k_{aA} = k_p$ one gets

$$\int\limits_0^R \mathrm{d}r\, u^2_{k_p l_B}(r) = i\,(-1)^{l_B+1} \tilde{C}^2_{l_B}/A_{l_B} - \frac{i}{2\,k_p}\, e^{2\,i\,\rho_p}. \tag{10}$$

Here $\rho_p = k_p R - \eta_p\, \ln(2k_p\, R)$. On the left-hand-side under the integral sign we have the function $u^2_{k_p l_B}(r)$, which is regular at $r = 0$ (see Eq. (5)).

Note that at the pole $k_{aA} = k_p$ $\;S^{-1}_{l_B}(k_p) = 0$ and one can see from Eq. (7) that in the external region the wave function $u_{k_p l_B}(R)$ satisfies the radiation condition:

$$u_{k_p l_B}(r) \overset{r>R_N}{=} \tilde{C}_{l_B}\, e^{i\rho_p}. \tag{11}$$

For the bound state $k_p = i\,\kappa_{aA}$ and

$$u_{i\,\kappa_{aA} l_B}(r) \overset{r>R_N}{=} C_{l_B}\, W_{-\eta^{bs}_{aA},\, l_B+1/2}(2\,k_p\, r) \overset{r\to\infty}{\approx} C_{l_B} e^{-\kappa_{aA}\, r - \eta^{bs}_{aA}\, \ln(2\,\kappa_{aA}\, r)}, \tag{12}$$

where $R_N$ is the $a-A$ nuclear interaction radius. For the resonance state $k_p = k_{aA(\mathcal{R})}$ and $u_{k_{aA(\mathcal{R})}l_B}(r)$ is the resonance Gamow wave function with the resonance energy $E_{aA(\mathcal{R})}$:

$$u_{k_{aA(\mathcal{R})}l_B}(r) \stackrel{r>R_N}{=} C_{l_B}\, W_{-i\,\eta^{(\mathcal{R})}_{aA},\, l_B+1/2}(-2\,i\,k_{aA(\mathcal{R})}\,r) \stackrel{r\to\infty}{\approx} e^{-\pi\,\eta^{(\mathcal{R})}_{aA}/2}\, C_{l_B} e^{i\,k_{aA(\mathcal{R})}\,r - i\,\eta^{(\mathcal{R})}_{aA}\,\ln(2\,k_{aA(\mathcal{R})}\,r)}$$
$$= \tilde{C}_{l_B} e^{i\,k_{aA(\mathcal{R})}\,r - i\,\eta^{(\mathcal{R})}_{aA}\,\ln(2\,k_{aA(\mathcal{R})}\,r)}. \tag{13}$$

Here, $\eta^{(\mathcal{R})}_{aA} = \frac{Z_a\,Z_A\,e^2\,\mu_{aA}}{k_{aA(\mathcal{R})}}$ is the $a+A$ Coulomb parameter of the resonance.

The constant $\tilde{C}_{l_B}$ is related to the ANC $C_{l_B}$ as $\tilde{C}_{l_B} = e^{-\pi\,\eta_p/2}\,C_{l_B}$, where $\eta_p =, \frac{Z_a\,Z_A\,e^2\,\mu_{aA}}{k_p}$. For the resonances one has

$$\tilde{C}_{l_B} = e^{-\pi\,\eta^{\mathcal{R}}_{aA}/2}\,C_{l_B} \tag{14}$$

and for the bound states

$$\tilde{C}_{l_B} = e^{i\,\pi\,\eta^{bs}_{aA}/2}\,C_{l_B}. \tag{15}$$

Note that $C_{l_B}$, which is real for the bound states, is the standard definition of the ANC for the bound states and will be used in this paper for the bound states.

For the bound states the asymptotic of the bound-state wave function is exponentially decaying and the bound-state wave function can be normalized. The Gamow wave function of the resonance state asymptotically oscillates and exponentially increasing. To normalize the Gamow wave function one can use Zeldovich regularization procedure [17] which is a particular case of the more general Abel regularization:

$$\lim_{\beta\to+0}\int\limits_0^\infty \mathrm{d}r e^{-\beta\,r^2}\,u^2_{k_{aA(\mathcal{R})}l_B}(r) = 1. \tag{16}$$

For the bound state one can take under the integral sign $\beta = 0$ and obtain the usual normalization procedure. For the resonance state one can take the limit $\beta \to 0$ only after performing the integration over $r$. Note that Zel'dovich normalization was introduced for exponentially decaying potentials. In Appendix is shown that Zel'dovich regularization procedure works even for the Coulomb potentials.

For any finite $R$ one can rewrite Eq. (16) as

$$\int\limits_0^R \mathrm{d}r\, u^2_{k_{aA(\mathcal{R})}l_B}(r) + \lim_{\beta\to+0}\int\limits_R^\infty \mathrm{d}r e^{-\beta\,r^2}\,u^2_{k_{aA(\mathcal{R})}l_B}(r) = 1. \tag{17}$$

Assume that $R$ is so large that one can use the asymptotic expression (11) and Eq. (81) of Appendix. It leads to

$$\int\limits_0^R \mathrm{d}r\, u^2_{k_{aA(\mathcal{R})}l_B}(r) = 1 - \frac{i}{2\,k_{aA(\mathcal{R})}}\tilde{C}^2_{l_B}\,e^{2\,i\,\rho_p}, \tag{18}$$

Comparing Eqs (10) and (18) one arrives to the final equation, which expresses the residue in the pole of the elastic scattering $S$-matrix in terms of the ANC:

$$A_{l_B} = -i^{2\,l_B+1}\,\tilde{C}^2_{l_B}. \tag{19}$$

Equation (19) is universal and valid for bound state poles and resonances. In terms of the standard ANC $C_{l_B}$ the residue in the resonance pole is

$$A_{l_B} = -i^{2\,l_B+1}\,e^{-\pi\,\eta^{(\mathcal{R})}_{aA}}\,C^2_{l_B} \tag{20}$$

and for the bound state is given by Eq. (2).

Now it will be shown how to relate the ANC $\tilde{C}_{l_B}$ to the resonance width $\Gamma_{aA}$ . Here the following definitions are used:

$$E_{aA(\mathcal{R})} = k^2_{aA(R)}/(2\,\mu_{aA}) = E_{aA(0)} - i\,\Gamma_{aA}/2, \qquad E_{aA(0)} = \left[k^2_{aA(0)} - (\mathrm{Im}k_{aA(\mathcal{R})})^2\right]/(2\,\mu_{aA}),$$
$$\Gamma_{aA} = 2\,k_{aA(0)}\,\mathrm{Im}k_{aA(\mathcal{R})}/\mu_{aA}. \tag{21}$$

One can write

$$S_{l_B}(k_{aA}) = e^{2\,i\,\delta^{pot}_{l_B}}\,\frac{(k_{aA}+k_p)(k_{aA}-k^*_p)}{(k_{aA}-k_p)(k_{aA}+k^*_p)}, \tag{22}$$

where $\delta^{pot}_{l_B}$ is the non-resonant scattering phase shift. At $k_p = k_{aA(\mathcal{R})}$ and at $k_{aA} \to k_{aA(\mathcal{R})}$

$$A_{l_B}(k_{aA}) = -2\,i\,k_{aA(\mathcal{R})}\,\gamma\,\left[(1+\gamma^2)^{1/4} + (1+\gamma^2)^{-1/4}\right]^{-1}\,e^{i[2\,\delta^{pot}_{l_B}(k_{aA(\mathcal{R})}) - 1/2\,arctan(\gamma)]}, \tag{23}$$

$\gamma = \frac{\Gamma_{aA}}{2\,E_{aA(0)}}$. Equation (23) expresses the residue of the $S$-matrix elastic scattering element in terms of the resonance energy and the resonance width for broad resonances.

Recovering now all the quantum numbers one gets for a narrow resonance ($\gamma << 1$) up to terms of order $\sim \gamma$

$$\left(\tilde{C}^B_{aA\,l_B\,j_B\,J_B}\right)^2 = i^{-2\,l_B}\,e^{i\,2\,\delta^p_{l_B\,j_B\,J_B}(k_{aA(0)})}\,\frac{\mu_{aA}\,\Gamma_{aA\,l_B\,j_B\,J_B}}{k_{aA(0)}}, \tag{24}$$

where $\Gamma_{aA\,l_B\,j_B\,J_B}$ is the resonance width, $\delta^p_{l_B\,j_B\,J_B}(k^0_{aA})$ is the potential (non-resonance) scattering phase shift at the real resonance relative momentum $k_{aA\,(0)}$. This equation is my desired equation, which relates the ANC of the narrow resonance to the resonance width.

The residue in the resonance pole with recovered all the quantum numbers is

$$A^{J_B}_{l_B\,j_B} = -i^{2\,l_B+1}\,(\tilde{C}^B_{aA\,l_B\,j_B\,J_B})^2. \tag{25}$$

For the Breit-Wigner resonance ($\mathrm{Im}k_{aA\,(\mathcal{R})} << \mathrm{Re}k_{aA\,(\mathcal{R})} = k_{aA\,(0)}$) Eq. (25) takes the form

$$A^{J_B}_{l_B\,j_B} = -i^{2\,l_B+1}\,e^{-\,\pi\,\eta_{aA(0)}}\,\left(C^B_{aA\,l_B\,j_B\,J_B}\right)^2 = -i^{2\,l_B+1}\,(\tilde{C}^B_{aA\,l_B\,j_B\,J_B})^2, \tag{26}$$

where $\eta_{aA(0)} = Z_a\,Z_A\,e^2\,\mu_{aA}/k_{aA\,(0)}$. In terms of the resonance width the residue of the elastic scattering $S$-matrix element in the resonance pole is

$$A^{J_B}_{l_B j_B} = -\,ie^{2\,i\,\delta^p_{l_B\,j_B\,J_B}(k^0_{aA})}\,\frac{\mu_{aA}}{k_{aA\,(0)}}\,\Gamma_{aA\,l_B j_B J_B}. \tag{27}$$

## III. ANCS AND OVERLAP FUNCTIONS

Equations obtained in the previous section, which express the residues of the $S$-matrix elastic element in terms of the ANCs of the bound states and resonances, provide the most general and model-independent definition of the ANCs. From other side, in the Schrödinger formalism of the wave functions the ANC is defined as the amplitude of the tail of the overlap function of the bound state wave functions of $B$, $A$ and $a$. The overlap function is given by

$$\begin{aligned} I_{aA}(\mathbf{r}_{aA}) &= <\psi_c\,|\,\varphi_B(\xi_A,\,\xi_a,\,\mathbf{r}_{aA})> \\ &= \sum_{l_B m_{l_B} j_B m_{j_B}} < J_A M_A\; j_B m_{j_B}|J_B M_B >< J_a M_a\, l_B m_{l_B}|j_B m_{j_B} > Y_{l_B m_{l_B}}(\widehat{\mathbf{r}}_{aA})\,I_{aA\;l_B j_B\,J_B}(r_{aA}). \end{aligned} \tag{28}$$

Here

$$\psi_c = \sum_{m_{j_B} m_{l_B} M_A M_a} < J_A M_A\; j_B m_{j_B}|J_B M_B >< J_a M_a\, l_B m_{l_B}|j_B m_{j_B} > \widehat{A}_{aA}\{\varphi_A(\xi_A)\,\varphi_a(\xi_a)\,Y_{l_B\,m_{l_B}}(\widehat{\mathbf{r}}_{aA})\} \tag{29}$$

is the two-body $a+A$ channel wave function in the $jj$ coupling scheme, $< j_1\,m_1\;j_2\,m_2|j\,m >$ is the Clebsch-Gordan coefficient, $\widehat{A}_{aA}$ is the antisymmetrization operator between the nucleons of nuclei $a$ and $A$; $\varphi_i(\xi_i)$ represents the fully antisymmetrized bound state wave function of nucleus $i$ with $\xi_i$ being a set of the internal coordinates including spin-isospin variables, $J_i$ and $M_i$ are the spin and its projection of nucleus $i$. Also $\mathbf{r}_{aA}$ is the radius vector connecting the centers of mass of nuclei $a$ and $A$, $\hat{\mathbf{r}}_{aA} = \mathbf{r}_{aA}/r_{aA}$, $Y_{l_B\,m_{l_B}}(\hat{\mathbf{r}}_{Aa})$ is the spherical harmonics, and $I_{aA\;l_B j_B J_B}(r_{Aa})$ is the radial overlap function. Notations of the spins and angular momenta are given in section II A. The summation over $l_B$ and $j_B$ is carried out over the values allowed by the angular momentum and parity conservation in the virtual process $B \to A + a$.

The radial overlap function is given by

$$I_{aA\ l_B j_B\ J_B}(r_{aA}) = < \hat{A}_{aA}\,\{\varphi_A(\xi_A)\,\varphi_a(\xi_a)\,Y_{l_B\,m_{l_B}}(\widehat{\mathbf{r}}_{aA})\}|\,\varphi_B(\xi_A,\,\xi_a;\,\mathbf{r}_{aA}) >$$
$$= \binom{A}{a}^{\frac{1}{2}} < \varphi_A(\xi_A)\,\varphi_a(\xi_a)\,Y_{l_B\,m_{l_B}}(\widehat{\mathbf{r}}_{aA})|\,\varphi_B(\xi_A,\,\xi_a;\,\mathbf{r}_{aA}) > . \tag{30}$$

Eq. (30) follows from a trivial observation that, because $\varphi_B$ is fully antisymmetrized, the antisymmetrization operator $\hat{A}_{aA}$ can be replaced by the factor $\binom{A}{a}^{\frac{1}{2}}$. In what follows, in contrast to Blokhintsev et al (1977), I absorb this factor into the radial overlap function.

The tail of the radial overlap function ($r_{aA} > R_{aA}$) in the case of the normal asymptotic behavior is given by

$$I_{aA\ l_B\,j_B\,J_B}(r_{aA}) = C^B_{aA\,l_B\,j_B\,J_B}\,\frac{W_{-\eta^{bs}_{aA},\,l_B+1/2}(2\,\kappa_{aA}r_{aA})}{r_{aA}} \xrightarrow{r_{aA}\to\infty} C^B_{aA\,l_B j_B J_B}\,\frac{e^{-\kappa_{aA}r_{aA}-\eta^{bs}_{aA}\ln(2\,\kappa_{aA}r_{aA})}}{r_{aA}}. \tag{31}$$

Formally the radial resonance overlap function for the Breit-Wigner resonance in the external region ($r_{aA} > R_{aA}$) can be obtained from Eq. (31) by the substitution $\kappa_{aA} = -i\,k_{aA\,(\mathcal{R})}$:

$$I_{aA\ l_B\,j_B\,J_B}(k_{aA(\mathcal{R})},\,r_{aA}) = C^B_{aA\,l_B\,j_B\,J_B}\,\frac{W_{-i\,\eta^{(\mathcal{R})}_{aA},\,l_B+1/2}(-2\,i\,k_{aA\,(\mathcal{R})}r_{aA})}{r_{aA}} \tag{32}$$
$$\xrightarrow{r_{aA}\to\infty} C^B_{aA\,l_B j_B J_B}\,\frac{e^{i\,k_{aA\,(\mathcal{R})}\,r_{aA}-i\,\eta^{(\mathcal{R})}_{aA}\ln(-2\,i\,k_{aA\,(\mathcal{R})}\,r_{aA})}}{r_{aA}}$$
$$= \tilde{C}^B_{aA\,l_B j_B J_B}\,\frac{e^{i\,k_{aA\,(\mathcal{R})}\,r_{aA}-i\,\eta^{(\mathcal{R})}_{aA}\ln(2\,k_{aA\,(\mathcal{R})}\,r_{aA})}}{r_{aA}}. \tag{33}$$

This asymptotic behavior agrees with the asymptotic behavior of the resonant Gamow wave function given by Eq. (13).

## IV. R-MATRIX WAVE FUNCTIONS

Because the microscopic overlap functions for mirror resonances and bound states are not available, in this paper I use internal resonance and bound-state wave functions calculated in the the potential model. If the mirror symmetry holds the bound-state and resonance wave functions of the mirror states should be very similar in the internal region where the resonance wave functions are real. However, both wave functions differ in the external region where the bound state wave functions exponentially decrease while the resonance wave functions at the resonance energies exponentially increase (see section III). In the Wronskian method, which is developed in this paper, one needs the wave functions in the internal region in which it is very convenient to use the $R$-matrix method. In the $R$-matrix method the resonant wave functions are normalized to unity in the internal region. The border of this region is determined by the point at which the radial derivative of the internal resonant wave function is equal to zero. If the resonant wave function has a few nodes, the border of the internal region is determined by the last point at which the radial derivative of the resonant wave function vanishes. To make the bound-state wave functions close to the resonant wave functions the former are also renormalized to unity in the internal region.

In the $R$-matrix approach the resonant wave function is considered at the real part of the resonance energy $E_{aA\,(0)}$. In this approach the internal wave function at real energies is real and behaves similarly to the bound state-wave function of the mirror state. At the $R$-matrix channel radius $R_{ch}$ and $E_{aA} = E_{aA(0)}$ the internal wave function coincides with the external one and is proportional to the outgoing wave $O_{l_B}(k_{aA(0)},\,R_{ch})$. Below I present the internal and external $R$-matrix wave functions considering single-level, single-channel case. Again, for simplicity, the particles are assumed to be spinless.

I start from the external $R$-matrix wave function at the partial wave $l_B$, which is given by [11, 19]

$$X^{(ext)(+)}_{l_B}(\mathbf{k}_{aA},\,\mathbf{r}_{aA}) = i^{l_B+1}\,\frac{2\,\pi}{k_{aA}\,r_{aA}}\,Y^*_{l_B\,m_{l_B}}(\hat{\mathbf{k}}_{aA})\,Y_{l_B\,m_{l_B}}(\hat{\mathbf{r}}_{aA})\,\big[I_{l_B} - S_{l_B}\,O_{l_B}(k_{aA},\,r_{aA})\big], \tag{34}$$

where

$$S_{l_B} = e^{-2\,i\,[\delta^{hs}_{l_B}-\sigma^C_{l_B}]}\left(1 + \frac{i\,\Gamma_{l_B}}{E_R - E_{aA} - \frac{i\,\Gamma_{l_B}}{2}}\right) \tag{35}$$

is the elastic scattering $S$-matrix at $E_{aA}$ near the real resonance energy $E_{aA(0)}$. $\sigma^C_{l_B}$ is the Coulomb scattering phase shift and $\delta^{hs}_{l_B}$ is the $R$-matrix hard-sphere scattering phase shift:

$$e^{-2i\,\delta^{hs}_{l_B}} = \frac{G_{l_B}(k_{aA},R_{ch}) - i\,F_{l_B}(k_{aA},R_{ch})}{G_{l_B}(k_{aA},R_{ch}) + i\,F_{l_B}(k_{aA},R_{ch})}, \tag{36}$$

$F_{l_B}(k_{aA},r_{aA})$ and $G_{l_B}(k_{aA},r_{aA})$ are the regular and singular Coulomb solutions, $R_{ch}$ is the $R$-matrix channel radius.

The outgoing wave is given by

$$O_{l_B}(k_{aA},r_{aA}) = \left(G_{l_B}(k_{aA},r_{aA}) + i\,F_{l_B}(k_{aA},r_{aA})\right) e^{-i\,\sigma^C_{l_B}}. \tag{37}$$

At $r_a = R_{ch}$

$$O_{l_B}(k_{aA},R_{ch}) = e^{i\,[\delta^{hs}_{l_B}-\sigma^C_{l_B}]}\sqrt{F^2_{l_B}(k_{aA},R_{ch}) + G^2_{l_B}(k_{aA},R_{ch})}. \tag{38}$$

$O_{l_B}(k_{aA},\,r_{aA})$ can be expressed it terms of the Whitteker function:

$$O_{l_B}(k_{aA},\,r_{aA}) = i^{-l_B}\,e^{\pi\,\eta_{aA/2}}\,W_{-i\eta_{aA},l_B+1/2}(-2\,i\,k_{aA}\,r_{aA}). \tag{39}$$

At $r_{aA} = R_{ch}$ and $E_{aA} = E_{aA(0)}$

$$X^{(ext)(+)}_{l_B}(\mathbf{k}_{aA(0)},\,\mathbf{R}_{ch}) = i^{l_B+1}\,\frac{4\,\pi}{k_{aA(0)}\,R_{ch}}\,e^{-2\,i\,[\delta^{hs}_{l_B}-\sigma^C_{l_B}]}\,Y^*_{l_B\,m_{l_B}}(\hat{\mathbf{k}}_{aA(0)})\,Y_{l_B\,m_{l_B}}(\hat{\mathbf{R}}_{ch})\,O_{l_B}(k_{aA(0))},R_{ch}). \tag{40}$$

The $R$-matrix internal resonant wave function in the partial wave $l_B$, in which the resonant is present, at energy $E_{aA}$ near the resonance is given by

$$X^{(int)(+)}_{l_B}(\mathbf{k}_{aA},\mathbf{r}_{aA}) = i^{l_B}\,\frac{2\,\pi}{k_{aA}\,r_{aA}}\sqrt{\frac{k_{aA}}{\mu_{aA}}}\,e^{-i\,[\delta^{hs}_{l_B}-\sigma^C_{l_B}]}\,Y^*_{l_B\,m_{l_B}}(\hat{\mathbf{k}}_{aA})\,Y_{l_B\,m_{l_B}}(\hat{\mathbf{r}}_{aA})\;\frac{\Gamma^{1/2}_{l_B}}{E_{\mathcal{R}} - E_{aA} - i\frac{\Gamma_{l_B}}{2}}\,\phi^{(int)}_{l_B}(k_{aA},r_{aA}). \tag{41}$$

The $R$-matrix internal resonant wave function $\phi^{(int)}_{l_B}(k_{aA},r_{aA})$ can be found as a solution of the Schrödinger equation with the two-body Woods-Saxon $V_{aA}$ potential. The $R$-matrix method will be used below for mirror resonance and bound states. I consider the loosely bound states which become the mirror resonances by replacing one of the neutrons by a proton. The considered binding energies and real energies of the mirror resonances are significantly smaller than the depth of the potential. That is why both mirror solutions of the Schrödinger equation should be very similar in the internal region where both solutions are real.

At $r_{aA} = R_{ch}$ and $E_{aA} = E_{aA(0)}$ (see Eq. (A(10)) from [11] in which the reduced width amplitude should be expressed in terms of the resonance width ) follows that

$$\phi^{(int)}_{l_B}(k_{aA(0)},R_{ch}) = \sqrt{\frac{\mu_{aA}\,\Gamma_{l_B}}{k_{aA(0)}}}\,e^{-i\,[\delta^{hs}_{l_B}-\sigma^C_{l_B}]}\,O_{l_B}(k_{aA(0)},R_{ch}). \tag{42}$$

Thus at the real part of the resonance energy $E_{aA} = E_{aA(0)}$ and $r_{aA} = R_{ch}$ the internal radial wave function $\phi^{(int)}_{l_B}(R_{ch})$ is proportional to the outgoing wave $O_{l_B}(k_{aA(0)},R_{ch})$. Equation (42) is also follows from the matching of the internal and external wave radial wave function, see below.

Taking into account Eq. (24) and that in the $R$-matrix approach the potential scattering phsse shift is $\delta_{l_B} = -(\delta^{hs}_{l_B} - \delta^C_{l_B})$ one gets

$$\phi^{(int)}_{l_B}(k_{aA(0)},R_{ch}) = C_{l_B}\,W_{-i\eta_{aA(0)},l_B+1/2}(-2\,i\,k_{aA(0)}\,R_{ch}), \tag{43}$$

$\eta_{aA(0)} = \frac{Z_a\,Z_A\,e^2\,\mu_{aA}}{k_{aA(0)}}$.

At $r_{aA} = R_{ch}$ and $E_{aA} = E_{aA(0)}$ one gets

$$X^{(int)(+)}_{l_B}(\mathbf{k}_{aA(0)},\mathbf{R}_{ch}) = i^{l_B+1}\,\frac{4\,\pi}{k_{aA}\,r_{aA}}\,e^{-2\,i\,[\delta^{hs}_{l_B}-\sigma^C_{l_B}]}\,Y^*_{l_B\,m_{l_B}}(\hat{\mathbf{k}}_{aA})\,Y_{l_B\,m_{l_B}}(\hat{\mathbf{R}}_{ch})\,O_{l_B}(k_{aA(0)},R_{ch}). \tag{44}$$

Thus at $r_{aA} = R_{ch}$ and $E_{aA} = E_{aA(0)}$ one gets matching of the internal and external $R$-matrix wave functions

$$X^{(ext)(+)}_{l_B}\mathbf{k}_{aA(0)}, \mathbf{R}_{ch}) = X^{(int)(+)}(\mathbf{k}_{aA(0)}, \mathbf{R}_{ch}) \tag{45}$$

and both wave functions are proportional to the outgoing wave $O_{l_B}(k_{aA}, R_{ch})$.

I can write the radial overlap function $I_{aA\ l_B\ j_B\ J_B}(k_{aA(0)},\ R_{ch})$ in terms of the outgoing wave $O_{l_B}(k_{aA(0)}, R_{ch})$ and the Whittaker function:

$$I_{aA\ l_B\ j_B\ J_B}(k_{aA(0)},\ R_{ch}) = \tilde{C}^B_{aA\,l_B\ j_B\ J_B}\ i^{l_B}\ \frac{O_{l_B}(k_{aA(0)},\ R_{ch})}{R_{ch}} = \sqrt{\frac{\mu_{aA}}{k_{aA(0)}}\,\Gamma_{aA\,l_B j_B J_B}}\ e^{-\,i\,[\delta^{hs}_{l_B} - \sigma^C_{l_B}]}\ \frac{O_{l_B}(k_{aA(0)}, R_{ch})}{R_{ch}}$$

$$= C^B_{aA\,l_B\ j_B\ J_B}\ \frac{W_{-i\eta_{aA(0)},l_B+1/2}(k_{aA(0)},\ R_{ch})}{R_{ch}}$$

$$= \ i^{-l_B}\ e^{-\,i\,[\delta^{hs}_{l_B} - \sigma^C_{l_B}]}\ e^{\pi\,\eta_{aA(0)}/2}\ \sqrt{\frac{\mu_{aA}}{k_{aA(0)}}\,\Gamma_{aA\,l_B j_B J_B}}\ \frac{W_{-i\eta_{aA(0)},l_B+1/2}(k_{aA(0)}R_{ch})}{R_{ch}}. \tag{46}$$

As one can see, the calculated in the $R$-matrix resonant radial overlap function at the channel radius $r_{aA} = R_{ch}$ and $E_{aA} = E_{aA(0)}$ is proportional to the the square root of the resonance width. It makes convenient to use the $R$-matrix method to determine the ratio of the resonance width and the bound-state ANC of the mirror states using the Wronskian method developed below.

## V. CONNECTION BETWEEN BREIT-WIGNER RESONANCE WIDTH AND ANC OF MIRROR RESONANCE AND BOUND STATES FROM PINKSTON-SATCHLER EQUATION

### A. ANC and Pinkston-Satchler equation

In [11] the relationship between the mirror proton and neutron ANCs was derived using the Pinkston-Satchler equation [20, 21]. Here I extend this derivation to obtain the ratio for the resonance width and the ANC of the mirror bound state in terms of the Wronskians, which follows from the Pinkston-Satchler equation.

First, using Pinkston-Satchler equation I derive the equation for the ANC of the narrow resonance state, which contains the source term [6, 22]. This derivation is valid for both bound and resonance state. That is why following [11] I start from the Schrödinger equation for the resonance scattering wave function at the real part E $_{aA(0)}$ of the resonance energy :

$$(E_{(0)} - \widehat{T}_A - \widehat{T}_a - \widehat{T}_{aA} - V_a - V_A - V_{aA})\Psi(\xi_A, \xi_a;\, \mathbf{r}_{aA}) = 0. \tag{47}$$

Here, $\widehat{T}_i$ is the internal motion kinetic energy operator of nucleus $i$, $\widehat{T}_{aA}$ is the kinetic energy operator of the relative motion of nuclei $a$ and $A$, $V_i$ is the internal potential of nucleus $i$ and $V_{aA}$ is the interaction potential between $a$ and $A$, $E_{(0)} = E_{aA(0)} - \varepsilon_a - \varepsilon_A$ is the total energy of the system $a + A$ in the continuum. The operator $E_{(0)} - \widehat{T}_A - \widehat{T}_a - \widehat{T}_{aA} - V_a - V_A - V_{aA}$ in Eq. (47) is symmetric over interchange of nucleons of $a$ and $A$, while $\Psi(\xi_a, \xi_A; \mathbf{r}_{aA})$ is antisymmetric, $\varepsilon_i$ is the total binding energy of nucleus $i$. Hence, by multiplying the Schrödinger equation (47) from the left by

$$\binom{A}{a}^{1/2} \sum_{m_{j_B} m_{l_B} M_A M_a} < J_A M_A\ j_B m_{j_B} | J_B M_B >< J_a M_a\, l_B m_{l_B} | j_B m_{j_B} > Y^*_{l_B m_{l_B}}(\widehat{\mathbf{r}}_{aA})\, \varphi_A(\xi_A)\, \varphi_a(\xi_a), \tag{48}$$

where the antisymmetrization operator $\hat{A}_{aA}$ in Eq. (48) is replaced by $\binom{A}{a}^{1/2}$, I get the equation for the radial overlap function with the source term $Q_{l_B j_B J_a J_A J_B}(r_{aA})$ [22]:

$$\left(E_{aA(0)} - \hat{T}_{r_{aA}} - V^{centr}_{l_B} - U^C_{aA}\right) I^B_{aA\ l_B\ j_B\ J_B}(r_{aA}) = Q_{l_B j_B J_a J_A J_B}(r_{aA}). \tag{49}$$

Here $\hat{T}_{r_{aA}}$ is the radial relative kinetic energy operator of the particles $a$ and $A$, $V^{centr}_{l_B}$ is the centrifugal barrier for the relative motion of $a$ and $A$ with the orbital momentum $l_B$. For charged particles it is convenient to single out the channel Coulomb interaction $U^C_{aA}(r_{aA})$ between the centers of mass of nuclei $a$ and $A$.

The source term is given by

$$Q_{l_B j_B J_a J_A J_B}(r_{aA}) = \sum_{m_{j_B} m_{l_B} M_A M_a} < J_A M_A \; j_B m_{j_B} | J_B M_B >< J_a M_a \, l_B m_{l_B} | j_B m_{j_B} >$$

$$\times \binom{A}{a}^{1/2} \int \mathrm{d}\,\Omega_{\mathbf{r}_{aA}} \; < \varphi_a(\xi_a)\, \varphi_A(\xi_A) | V_{aA} - U^C_{aA} | Y^*_{l_B m_{l_B}}(\widehat{\mathbf{r}}_{aA}) \Psi(\xi_a, \xi_A; \mathbf{r}_{aA}) > . \tag{50}$$

The integration in the matrix element $< \varphi_a(\xi_a)\, \varphi_A(\xi_A) | V_{aA} - U^C_{aA} | Y^*_{l_B m_{l_B}}(\widehat{\mathbf{r}}_{aA}) \Psi(\xi_a, \xi_A; \mathbf{r}_{aA}) >$ in Eq. (50) is carried out over all the internal coordinates of nuclei $a$ and $A$.

Owing to the presence of the short-range potential operator $V_{aA} - U^C_{aA}$ (potential $V_{aA}$ is the sum of the nuclear $V^N_{aA}$ and the Coulomb $V^C_{aA}$ potentials and subtraction of $U^C_{aA}$ removes the long-range Coulomb term from $V_{aA}$) the source term is also a short-range function. Then Eq. (49) for the radial overlap function can be rewritten as

$$I_{aA\; l_B\, j_B\, J_B}(k_{aA(0)},\, r_{aA}) = \frac{1}{R_{aA}} \int\limits_0^{R_{aA}} \mathrm{d}r'_{aA}\, r'_{aA}\, G^C_{l_B}(r_{aA},\, r'_{aA}; E_{aA(0)})\, Q_{l_B j_B J_a J_A J_B}(r'_{aA}), \tag{51}$$

where $R_{aA}$ is the $a - A$ nuclear interaction radius. In the $R$-matrix approach $R_{aA}$ can be replaced by the channel radius $R_{ch}$, which can be varied.

Equation (51) is of fundamental importance because it allows one to express the radial overlap function in terms of the internal wave function of the nucleus $B$.

The partial Coulomb two-body Green function is given by [23]

$$G^C_{l_B}(r_{aA}, r'_{aA}; E_{aA}) = -2\,\mu_{aA}\, \frac{\varphi^C_{l_B}(k_{aA},\, r_{aA<})\, f^{C(+)}_{l_B}(k_{aA},\, r_{aA>})}{L^{C(+)}_{l_B}}, \tag{52}$$

where $r_{aA<} = \min\{r_{aA}, r'_{aA}\}$ and $r_{aA>} = \max\{r_{aA}, r'_{aA}\}$. The Coulomb regular solution $\varphi^C_{l_B}(k_{aA},\, r_{aA})$ of the partial Schrödinger equation at real momentum $k_{aA}$ is

$$\begin{aligned}
&\varphi^C_{l_B}(k_{aA},\, r_{aA}) = \frac{1}{2\,i\,k_{aA}} \left[ L^{C(-)}_{l_B}(k_{aA})\, f^{C(+)}_{l_B}(k_{aA},\, r_{aA}) - L^{C(+)}_{l_B}(k_{aA})\, f^{C(-)}_{l_B}(k_{aA},\, r_{aA}) \right] \\
&= r^{l_B+1}_{aA}\, e^{i\,k_{aA}\,r_{aA}}\; {}_1F_1(l_B + 1 + i\eta_{aA}, 2\,l_B + 2; -2\,i\,k_{aA}\,r_{aA}) \\
&= e^{-i\,\pi\,l_B/2}\, L^{C(+)}_{l_B}(k_{aA})\, \frac{e^{i\,\sigma^C_{l_B}}\, F_{l_B}(k_{aA},\, r_{aA})}{k_{aA}},
\end{aligned} \tag{53}$$

where

$$e^{i\,\sigma^C_{l_B}}\, F_{l_B}(k_{aA}, r_{aA}) = e^{-\pi\,\eta_{aA}/2}\, \frac{\Gamma(l_B + 1 + \,i\,\eta_{aA})}{2\,\Gamma(2\,l_B + 2)}\, (2\,k_{aA}\,r_{aA})^{l_B+1}\, e^{i\,k_{aA}\,r_{aA}}\; {}_1F_1(l_B + 1 + i\,\eta_{aA}, 2\,l_B + 2;\; -i\,2\,k_{aA}\,r_{aA}), \tag{54}$$

$\sigma^C_{l_B}$ is the Coulomb scattering phase shift. Also

$$f^{C(\pm)}_{l_B}(k_{aA}, r_{aA}) = e^{\pi\,\eta_{aA}/2}\, W_{\mp i\,\eta_{aA},\, l_B+1/2}(\mp 2\,i k_{aA}\,r_{aA}) \tag{55}$$

are the Jost solutions (singular at the origin $r_{aA} = 0$),

$$L^{C(\pm)}_{l_B}(k_{aA}) = \frac{1}{(2\,k_{aA})^{l_B}}\, e^{\pi\,\eta_{aA}/2}\, e^{\pm i\,\pi\,l_B/2}\, \frac{\Gamma(2\,l_B + 2)}{\Gamma(l_B + 1 \pm i\,\eta_{aA})} \tag{56}$$

are the Jost functions.

Iit is convenient to introduce the modified Coulomb wave function

$$\tilde{\varphi}^C_{l_B}(k_{aA},\, r_{aA}) = \frac{\varphi^C_{l_B}(k_{aA},\, r_{aA})}{L^{C(+)}_{l_B}(k_{aA})}, \tag{57}$$

which will be used from now on instead of $\varphi^C_{l_B}(k_{aA},\, r_{aA})$.

Let me use now the $R$-matrix method in which I replace $R_{aA}$ by $R_{ch}$. Then assuming in Eq. (51) $r_{aA} = R_{ch} + i0$ and taking into account Eq. (46) and (55) I get

$$\tilde{C}_{l_B} = i^{-l_B}\, e^{-\,i\,[\delta^{hs}_{l_B} - \sigma^C_{l_B}]}\, \sqrt{\frac{\mu_{aA}}{k_{aA(0)}}\,\Gamma_{aA\,l_B j_B J_B}} = 2\,\mu_{aA} \int\limits_0^{R_{ch}} \mathrm{d}r'_{aA}\, r'_{aA}\, \tilde{\varphi}^C_{l_B}(k_{aA(0)},\, r'_{aA})\, Q_{l_B j_B J_a J_A J_B}(r'_{aA}). \tag{58}$$

Using Eqs. (53) and (57) one gets

$$e^{-\,i\,\delta^{hs}_{l_B}}\, \sqrt{\frac{\mu_{aA}}{k_{aA(0)}}\,\Gamma_{aA\,l_B j_B J_B}} = 2\,\frac{\mu_{aA}}{k_{aA(0)}} \int\limits_0^{R_{ch}} \mathrm{d}r'_{aA}\, r'_{aA}\, F_{l_B}(k_{aA(0)},\, r'_{aA})\, Q_{l_B j_B J_a J_A J_B}(r'_{aA}). \tag{59}$$

This equation provides the ANC or resonance width of the narrow resonance, which may depend on the channel radius $R_{ch}$. Here I am interested in the ratio of the resonance width and the square of the ANC of the mirror resonant and bound state. Below will be checked the sensitivity of this ratio to the variation of the channel radius.

### B. ANC in terms of Wronskian

The advantage of Eq. (59) is that to calculate the ANC one needs to know the microscopic resonant wave functions only in the nuclear interior where the *ab initio* methods like the no-core-shell-model [24–26], and the coupled-cluster method [27] are more accurate than in the external region. That is why Eq. (59) is so important if microscopic resonant wave functions are available. Now I will show that the radial integral in Eq. (59) can be transformed into the Wronskian at $r_{aA} = R_{aA}$. The philosophy of this transformation is the same as in the surface integral formalism [5, 11].

First, let us rewrite

$$V_{aA} - U^C_{aA} = V + V^{centr}_{l_B} - V_a - V_A - V^{centr}_{l_B} - U^C_{aA} \tag{60}$$

and take into account equations

$$(E_{aA(0)} - \hat{T}_a - \hat{T}_A - \hat{T}_{r_{aA}})\, \tilde{\varphi}^C_{l_B}(k_{aA(0)},\, r_{aA})\, \varphi_a(\xi_a)\, \varphi_A(\xi_A) = (U^C_{aA} + V^{centr}_{l_B} + V_a + V_A)\, \tilde{\varphi}^C_{l_B}(k_{aA(0)},\, r_{aA})\, \tilde{\varphi}_a(\xi_a)\, \varphi_A(\xi_A) \tag{61}$$

and

$$(E_{aA(0)} - \hat{T}_a - \hat{T}_A - \hat{T}_{r_{aA}}) < Y_{l_B m_{l_B}}(\widehat{\mathbf{r}}_{aA}) | \Psi(\xi_a,\, \xi_A;\, \mathbf{r}_{aA} > = (V_{aA} + V_a + V_A + V^{centr}_{l_B}) < Y_{l_B m_{l_B}}(\widehat{\mathbf{r}}_{aA}) | \Psi(\xi_a,\, \xi_A;\, \mathbf{r}_{aA} >, \tag{62}$$

where $\hat{T}_{r_{aA}}$ is the radial kinetic energy operator.

Then we get

$$\tilde{C}^B_{aA\;l_B\,j_B\,J_B} \approx -\,2\,\mu_{aA} \int\limits_0^{R_{aA}} \mathrm{d}r_{aA}\, r_{aA}\, \tilde{\varphi}^C_{l_B}(k_{aA(0)},\, r_{aA})\, Q_{l_B j_B J_a J_A J_B}(r_{aA}) = -\,2\,\mu_{aA}$$

$$\times \sum_{m_{j_B} m_{l_B} M_A M_a} < J_A M_A\; j_B m_{j_B} | J_B M_B > < J_a M_a\, l_B m_{l_B} | j_B m_{j_B} > \binom{A}{a}^{1/2} \int\limits_0^{R_{aA}} \mathrm{d}r_{aA}\, r_{aA}\, \tilde{\varphi}^C_{l_B}(k_{aA(0)},\, r_{aA})$$

$$\times \int \mathrm{d}\,\Omega_{\mathbf{r}_{r_{aA}}} < \varphi_a(\xi_a)\, \varphi_A(\xi_A) | \overleftarrow{\hat{T}}_{r_{aA}} + \overleftarrow{\hat{T}}_a + \overleftarrow{\hat{T}}_A - \overrightarrow{\hat{T}}_a - \overrightarrow{\hat{T}}_A - \overrightarrow{\hat{T}}_{r_{aA}} | Y^*_{l_B m_{l_B}}(\widehat{\mathbf{r}}_{aA})\, \Psi(\xi_a, \xi_A; \mathbf{r}_{aA}) >$$

$$= -\,2\,\mu_{aA} \sum_{m_{j_B} m_{l_B} M_A M_a} < J_A M_A\; j_B m_{j_B} | J_B M_B > < J_a M_a\, l_B m_{l_B} | j_B m_{j_B} >$$

$$\times \binom{A}{a}^{1/2} \int\limits_0^{R_{aA}} \mathrm{d}r_{aA}\, r_{aA}\, \tilde{\varphi}^C_{l_B}(k_{aA(0)},\, r_{aA}) \int \mathrm{d}\,\Omega_{\mathbf{r}_{aA}} < \varphi_a(\xi_a)\, \varphi_A(\xi_A) | \overleftarrow{\hat{T}}_{r_{aA}} - \overrightarrow{\hat{T}}_{r_{aA}} | Y^*_{l_B m_{l_B}}(\widehat{\mathbf{r}}_{aA}) \Psi(\xi_a, \xi_A; \mathbf{r}_{aA}) >$$

$$= -\,2\,\mu_{aA} \int\limits_0^{R_{aA}} \mathrm{d}r_{aA}\, r_{aA}\, \tilde{\varphi}^C_{l_B}(k_{aA(0)},\, r_{aA}) \left(\overleftarrow{\hat{T}}_{r_{aA}} - \overrightarrow{\hat{T}}_{r_{aA}}\right) I_{aA\;l_B\,j_B\,J_B}(k_{aA(0)},\, r_{aA}). \tag{63}$$

Here $R_{aA}$ is the $a-A$ nuclear interaction radius. In the $R$-matrix approach $R_{aA}$ can be replaced by the channel radius $R_{ch}$ which can be varied.

Taking into account that

$$f(x)\left(\frac{\overleftarrow{d}^2}{dx^2}-\frac{\overrightarrow{d}^2}{dx^2}\right)g(x = \frac{d}{dx}\left(g(x)\,\frac{df(x)}{dx}-f(x)\,\frac{dg(x)}{dx}\right) \tag{64}$$

we arrive at the final expression for the ANC of the resonance state in terms of the Wronskian:

$$\tilde{C}^B_{aA\ l_B\,j_B\,J_B} = \mathcal{W}[I_{aA\ l_B\,j_B\,J_B}(k_{aA(0)},\,r_{aA}),\,\tilde{\varphi}^C_{l_B}(k_{aA(0)},\,r_{aA})]\Big|_{r_{aA}=R_{ch}}, \tag{65}$$

where the Wronskian

$$\begin{aligned}&\mathcal{W}[\,I_{aA\ l_B\,j_B\,J_B}(r_{aA}),\,\tilde{\varphi}^C_{l_B}(k_{aA(0)},\,r_{aA})]\\ &= I_{aA\ l_B\,j_B\,J_B}(k_{aA(0)},\,r_{aA})\,\frac{\mathrm{d}\tilde{\varphi}^C_{l_B}(k_{aA(0)},\,r_{aA})}{\mathrm{d}r_{aA}}-\tilde{\varphi}^C_{l_B}(k_{aA(0)},\,r_{aA})\,\frac{\mathrm{d}I_{aA\ l_B\,j_B\,J_B}(k_{aA(0)},\,r_{aA})}{\mathrm{d}r_{aA}}.\end{aligned} \tag{66}$$

I would like to underscore that Eq. (65) has been derived by transforming the internal integral into the Wronskian at the channel radius $R_{ch}$. Note that at too small radii $R_{ch}$ the Wronskian $\mathcal{W}[\,I_{aA\ l_B\,j_B\,J_B}(r_{aA}),\,\tilde{\varphi}^C_{l_B}(k_{aA(0)},\,r_{aA})]$ depends on the radius but the sensitivity to the radius decreases as $R_{ch}$ increases.

There is another more direct derivation of Eq. (65) . We know that the Wronskian calculated for two independent solutions of the Schrödinger equation is a constant [23]. In the $R$-matrix approach the internal radial overlap function $I_{aA\ l_B\,j_B\,J_B}(k_{aA(0)},\,r_{aA})$ at $r_{aA}\to R_{ch}$ behaves like the Whittaker function, see Eq. (46), and is given by

$$I_{aA\ l_B\,j_B\,J_B}(k_{aA(0)},\,r_{aA}) = \tilde{C}^B_{aA\,l_B\,j_B\,J_B}\,\frac{f^{C(+)}_{l_B}(k_{aA(0)},r_{aA})}{R_{ch}}. \tag{67}$$

This Whittaker function is a singular solution of the radial Schrödinger equation. $\tilde{\varphi}^C_{l_B}(k_{aA(0)},\,r_{aA})$ is an independent regular solution of the same equation. Taking into account that $\mathcal{W}[\,f^{C(+)}_{l_B}(k_{aA(0)},\,r_{aA}),\,f^{C(-)}_{l_B}(k_{aA(0)},r_{aA})] = -2\,i\,k_{aA(0)}$ and Eq. (53) one gets at $r_{aA}=R_{ch}$

$$\mathcal{W}[I_{aA\ l_B\,j_B\,J_B}(k_{aA(0)},\,r_{aA}),\,\tilde{\varphi}^C_{l_B}(k_{aA(0)},\,r_{aA})]\Big|_{r_{aA}=R_{ch}} = \tilde{C}^B_{aA\ l_B\,j_B\,J_B}. \tag{68}$$

Note that the constancy of the Wronskian only applies to local potentials. But here one needs this only at large distances, where zero potentials are local anyway.

I will demonstrate that the Wronskian $\mathcal{W}[I_{aA\ l_B\,j_B\,J_B}(k_{aA(0)},\,r_{aA}),\,\tilde{\varphi}^C_{l_B}(k_{aA(0)},\,r_{aA})]\Big|_{r_{aA}=R_{aA}}$ depends on $R_{ch}$ and reaches a constant value, which is equal to the ANC of the resonance state, when $R_{ch}$ increases.

My idea is to use Eq. (65) to calculate the Wronskian $\mathcal{W}[I_{aA\ l_B\,j_B\,J_B}(k_{aA(0)},\,r_{aA}),\,\tilde{\varphi}^C_{l_B}(k_{aA(0)},\,r_{aA})]\Big|_{r_{aA}=R_{aA}}$ at the channel radii which are smaller than the radius of nucleus $B=(aA)$, and gradually increase $R_{ch}$ until the Wronskian reaches its constant value. In the nuclear interior the contemporary microscopic models can provide quite accurate overlap functions. The sensitivity to the variation of the channel radius of the ratio of the ANCs of the resonance and mirror bound state is significantly weaker than that of the individual ANCs (or, equivalently, of the resonance width and the bound state ANC) of the mirror states.

## VI. RATIO OF RESONANCE WIDTH AND ANC OF MIRROR BOUND STATE

### A. Three different equations

In this part three different equations for the ratio of the resonance width and the ANC of the mirror bound state are presented. Let $B_1=(a_1\,A_1)$ and $B_2=(a_2\,A_2)$ be mirror nuclei. Then the quantum numbers in both nuclei are the same. We also assume that the channel radius $R_{ch}$ is the same for both mirror nuclei. The ratio of the ANCs of

the mirror resonance and bound states is given by the ratio of the corresponding Wronskians. Taking into account Eq. (65) one gets for the ratio of the resonance width and the bound state ANC for mirror states:

$$\frac{\Gamma_{a_1A_1\ l_B\,j_B\,J_B}}{(C^{B_2}_{a_2\,A_2\ l_B\,j_B\,J_B})^2} = \sqrt{\frac{2\,E_{a_1A_1(0)}}{\mu_{a_1A_1}}}\,\frac{\Big|\mathcal{W}[I_{a_1A_1\ l_B\,j_B\,J_B}(k_{a_1A_1(0)},\,r_{a_1A_1}),\,\tilde{\varphi}^C_{l_B}(k_{a_1A_1(0)},\,r_{a_1A_1})]\Big|^2\Big|_{r_{a_1A_1}=R_{ch}}}{\Big(\mathcal{W}[I_{a_2A_2\ l_B\,j_B\,J_B}(\kappa_{a_2A_2},\,r_{a_2A_2}),\,\tilde{\varphi}^C_{l_B}(i\kappa_{a_2A_2},\,r_{a_2A_2})]\Big)^2\Big|_{r_{a_2A_2}=R_{ch}}}, \tag{69}$$

where $E_{a_1A_1(0)}$ and $\mu_{aA}$ are expressed in MeV. Equation (69) allows one to determine the resonance width if the ANC of the mirror bound state is known and vice versa.

To calculate the ratio $\frac{\Gamma^{B_1}_{a_1A_1\ l_B\,j_B\,J_B}}{(C^{B_2}_{a_2\,A_2\ l_B\,j_B\,J_B})^2}$ one needs the microscopic radial overlap functions. If these radial overlap functions are not available then one can use a standard approximation for the overlap functions:

$$I_{a_1A_1\ l_B\,j_B\,J_B}(k_{a_1A_1(0)},\,r_{aA}) \approx S^{1/2}_{a_1A_1}\,\varphi_{a_1A_1\ l_B\,j_B\,J_B}(k_{a_1A_1(0)},\,r_{a_1A_1}), \tag{70}$$

$$I_{a_2A_2\ l_B\,j_B\,J_B}(\kappa_{a_2A_2},\,r_{aA}) \approx S^{1/2}_{a_2A_2}\,\varphi_{a_2A_2\ l_B\,j_B\,J_B}(\kappa_{a_2A_2},\,r_{a_2A_2}), \tag{71}$$

where $S_{a_1A_1}$ and $S_{a_2A_2}$ are the spectroscopic factors of the mirror resonance and bound states $(a_1A_1)$ and $(a_2A_2)$, respectively. $\varphi_{a_1A_1\ l_B\,j_B\,J_B}(k_{a_1A_1(0)},\,r_{a_1A_1})$ is a real internal resonant wave function calculated in the two-body model $(a_1\,A_1)$ using some phenomenological potential, for example, Woods-Saxon one, which supports the resonance state under consideration. $\varphi_{a_2A_2\ l_B\,j_B\,J_B}(\kappa_{a_2A_2},\,r_{a_2A_2})$ is the two-body bound-state wave function of the bound state $(a_2\,A_2)$, which is also calculated using the same nuclear potential as the mirror resonance state. If the mirror symmetry holds then $S_{a_1A_1} \approx S_{a_2A_2}$ and one gets an approximated $\frac{\Gamma_{a_1A_1\ l_B\,j_B\,J_B}}{(C^{B_2}_{a_2\,A_2\ l_B\,j_B\,J_B})^2}$ ratio in terms of the Wronskians, which does not contain the overlap functions:

$$\frac{\Gamma_{a_1A_1\ l_B\,j_B\,J_B}}{(C^{B_2}_{a_2\,A_2\ l_B\,j_B\,J_B})^2} \approx \sqrt{\frac{2\,E_{a_1A_1(0)}}{\mu_{a_1A_1}}}\,\frac{\Big|\mathcal{W}[\varphi_{a_1A_1\ l_B\,j_B\,J_B}(k_{a_1A_1(0)},\,r_{a_1A_1}),\,\tilde{\varphi}^C_{l_B}(k_{a_1A_1(0)},\,r_{a_1A_1})]\Big|^2\Big|_{r_{a_1A_1}=R_{ch}}}{\Big(\mathcal{W}[\varphi_{a_2A_2\ l_B\,j_B\,J_B}(\kappa_{a_2A_2},\,r_{a_2A_2}),\,\tilde{\varphi}^C_{l_B}(i\,\kappa_{a_2A_2},\,r_{a_2A_2})]\Big)^2\Big|_{r_{a_2A_2}=R_{ch}}}. \tag{72}$$

Meantime in [10] another expression for the mirror nucleon ANCs ratio was obtained another equation which provides the easiest way to determine $\frac{\Gamma_{a_1A_1\ l_B\,j_B\,J_B}}{(C^{B_2}_{a_2\,A_2\ l_B\,j_B\,J_B})^2}$. I will show here a simple way of the derivation of the ratio $\frac{\Gamma_{a_1A_1\ l_B\,j_B\,J_B}}{(C^{B_2}_{a_2\,A_2\ l_B\,j_B\,J_B})^2}$ from [10]. First, as it was pointed out in [10], in the nuclear interior the Coulomb interaction varies very little in the nuclear interior and its effect leads only to shifting of the energy of the bound state to the continuum. Hence, it can be assumed that $\tilde{\varphi}^C_{l_B}(k_{a_1A_1(0)},\,r_{a_1A_1})$ and $\tilde{\varphi}^C_{l_B}(i\,\kappa_{a_2A_2}\,r_{a_2A_2})$ behave similarly in the nuclear interior except for the overall normalization, that is

$$\tilde{\varphi}^C_{l_B}(k_{a_1A_1(0)},\,r_{aA}) = \frac{\tilde{\varphi}^C_{l_B}(k_{a_1A_1(0)},R_{ch})}{\tilde{\varphi}^C_{l_B}(\,i\,\kappa_{a_2A_2},\,R_{ch})}\,\tilde{\varphi}^C_{l_B}(i\,\kappa_{a_2A_2},\,r_{a_2A_2}). \tag{73}$$

Then

$$\frac{\Gamma_{a_1A_1\ l_B\,j_B\,J_B}}{(C^{B_2}_{a_2\,A_2\ l_B\,j_B\,J_B})^2} \approx \sqrt{\frac{2\,E_{a_1A_1(0)}}{\mu_{a_1A_1}}}\,\Big(\frac{\tilde{\varphi}^C_{l_B}(k_{a_1A_1(0)},R_{ch})}{\tilde{\varphi}^C_{l_B}(i\,\kappa_{a_2A_2},\,R_{ch})}\Big)^2$$
$$\times\,\frac{|\mathcal{W}[\varphi_{a_1A_1\ l_B\,j_B\,J_B}(k_{a_1A_1(0)},\,r_{a_1A_1}),\,\tilde{\varphi}^C_{l_B}(i\,\kappa_{a_2A_2},r_{a_2A_2})]\,|^2\,|_{r_{a_1A_1},\,r_{a_2A_2}=R_{ch}}}{\big(\mathcal{W}[\varphi_{a_2A_2\ l_B\,j_B\,J_B}(\kappa_{a_2A_2},\,r_{a_2A_2}),\,\tilde{\varphi}^C_{l_B}(i\,\kappa_{a_2A_2},\,r_{a_2A_2})]\big)^2\,|_{r_{a_2A_2}=R_{ch}}}. \tag{74}$$

Neglecting further the difference between the mirror wave functions $\varphi_{a_1A_1\ l_B\,j_B\,J_B}(k_{a_1A_1(0)},\,r_{a_1A_1})$ and $\varphi_{a_2A_2\ l_B\,j_B\,J_B}(\kappa_{a_2A_2},\,r_{a_2A_2})$ in the nuclear interior we obtain the approximate expression for $\frac{\Gamma_{a_1A_1\ l_B\,j_B\,J_B}}{(C^{B_2}_{a_2\,A_2\ l_B\,j_B\,J_B})^2}$ from [10] (in the notations of the current paper):

$$\frac{\Gamma_{a_1A_1\ l_B\,j_B\,J_B}}{(C^{B_2}_{a_2\,A_2\ l_B\,j_B\,J_B})^2} \approx \sqrt{\frac{2\,E_{a_1A_1(0)}}{\mu_{a_1A_1}}}\,\Big(\frac{\tilde{\varphi}^C_{l_B}(k_{a_1A_1(0)},\,R_{ch})}{\tilde{\varphi}^C_{l_B}(i\,\kappa_{a_2A_2},\,R_{ch})}\Big)^2. \tag{75}$$

In descending accuracy I can rank Eq. (69) as the most accurate. Taking into account that the microscopic overlap functions (calculated in the no-core-shell-model [24–26] or oscillator shell-model [28]) are accurate in the nuclear interior, using Eq (69) one can determine the ratio $\frac{\Gamma_{a_1A_1\ l_B\,j_B\,J_B}}{(C^{B_2}_{a_2\,A_2\ l_B\,j_B\,J_B})^2}$ quite accurately. Then follows Eq. (72) and finally Eq. (75). Note that Eq. (75) is valid only in the region where the mirror resonant and bound state wave functions do coincide or very close. The advantage of this equation is that it allows one to calculate the ratio without using the mirror wave functions and extremely simple to use.

Because for the cases under consideration the internal microscopic resonance wave functions are not available, in this paper the $\frac{\Gamma_{a_1A_1\ l_B\,j_B\,J_B}}{(C^{B_2}_{a_2\,A_2\ l_B\,j_B\,J_B})^2}$ ratio is calculated using Eqs (72) and (75). It allows one to determine the accuracy of both equations.

Note that the dimension of the ratio $\frac{\Gamma_{a_1A_1\ l_B\,j_B\,J_B}}{(C^{B_2}_{a_2\,A_2\ l_B\,j_B\,J_B})^2}$ is determined by the ratio $\frac{2\,E_{a_1A_1(0)}}{\mu_{a_1A_1}}$. To make it dimensionless I assume that the reduced mass $\mu_{a_1A_1}$ and the real part of the resonance energy $E_{a_1A_1(0)}$ are expressed in MeV.

### B. R-matrix wave function

Because the microscopic overlap functions for mirror resonances are not available, in this paper I use internal resonance and bound-state wave functions calculated in the the potential model at real energies. In the developed Wronskian method one needs the wave functions in the internal region in which it is very convenient to use the $R$-matrix method. In the $R$-matrix approach the resonant wave function is considered at the real part of the resonance energy $E_{aA\,(0)}$ and is real in the internal region. If the mirror symmetry holds the bound-state and resonance wave functions of the mirror states should be very similar in the internal region. The $R$-matrix resonant wave function is normalized to unity in the internal region. The border of this region is determined by the point at which the radial derivative of the internal resonant wave function is equal to zero. If the resonant wave function has a few nodes, the border of the internal region is determined by the last point at which the radial derivative of the resonant wave function vanishes. The bound-state wave function is normalized to unity in the whole coordinate space. To make the bound-state wave function close to the resonant wave function the former is also renormalized to unity in the internal region. The advantage of the Wronskian method is that to calculate the ratio of the resonance width and the ANC of the mirror states one can use the internal real resonant and bound-state wave functions.

## VII. COMPARISON OF RESONANCE WIDTHS AND ANCS OF MIRROR STATES

In this section a few examples of the application of Eqs. (72) and (75) are presented. To simplify the notations from now on the quantum numbers in the notations for the resonance width and the ANC are dropped and just use simplified notations, $\Gamma_{a_1A_1}$ and $C_{a_2\,A_2}$. Equation (72) gives $\Gamma_{a_1A_1}/(C_{a_2\,A_2})^2$ in terms of the ratio of the Wronskians and provides an exact value for given two-body mirror resonant and bound-state wave functions. Equation (75) gives the $\Gamma_{a_1A_1}/(C_{a_2\,A_2})^2$ ratio in terms of the Coulomb scattering wave functions at the real resonance momentum $k_{a_1A_1(0)}$ and the imaginary momentum of the bound state $i\,\kappa_{a_2A_2}$ at the channel radius $R_{ch}$. Hence, to determine the ratio $\Gamma_{a_1A_1}/(C_{a_2\,A_2})^2$ using Eq. (75) one does not need to know the mirror resonant and bound-state wave functions. However, to use this equation one should check whether the mirror wave functions are close. In calculations I deliberately increase the channel radius $R_{ch}$ to demonstrate the convergence of the calculated ratio $\Gamma_{a_1A_1}/(C_{a_2\,A_2})^2$ as $R_{ch}$ increases.

### A. Comparison of resonance width for $^{13}$N($\mathbf{2s_{1/2}}$) $\to$ $^{12}$C($\mathbf{0.0}$ MeV) + p and mirror ANC for virtual decay $^{13}$C($\mathbf{2s_{1/2}}$) $\to$ $^{12}$C($\mathbf{0.0}$ MeV) + n

I begin from the analysis of the isobaric analogue states $2s_{1/2}$ in the mirror nuclei $^{13}$N and $^{13}$C. The resonance energy of $^{13}$N($2s_{1/2}$) is $E_{p^{12}\mathrm{C}(0)} = 0.421$ MeV with the resonance width of $\Gamma_{p^{12}\mathrm{C}} = 0.0317 \pm 0.0008$ MeV [29]. The neutron binding energy of the mirror state $^{13}$C($2s_{1/2}$) is $\varepsilon_{n^{12}\mathrm{C}} = 1.8574$ MeV with the experimental ANC $C^2_{n^{12}\mathrm{C}} = 3.65$ fm$^{-1}$ [30, 31]. The experimental ratio $\Gamma_{p^{12}\mathrm{C}}/(C_{n^{12}\mathrm{C}})^2 = (4.40 \pm 0.57) \times 10^{-5}$ allows us to check the accuracy of both used equations. Because the dimension of the bound-state ANC is fm$^{-1/2}$ to get the dimensionless ratio I calculated $\Gamma_{p^{12}\mathrm{C}}/[\hbar\,c(C_{n^{12}\mathrm{C}})^2]$.

In Fig. 1 are shown the radial wave functions of the mirror states. Following the $R$-matrix procedure, both wave functions are normalized to unity over the internal volume with the radius $R_{ch} = 4.0$ fm. We see that the mirror

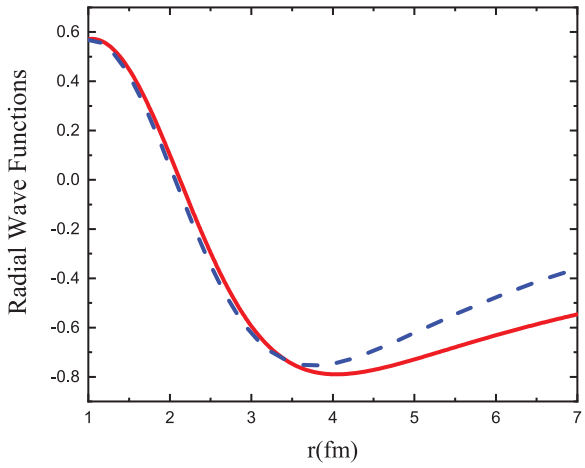


FIG. 1: Solid red line: the radial wave function of the $(p^{12}\mathrm{C})_{2s^+_{1/2}}$ resonance state; dashed blue line: the radial wave function of the mirror $(n^{12}\mathrm{C})_{2s^+_{1/2}}$ bound-state. $r$ is the distance between $N$, where $N = p, n$, and the c.m. of $^{12}$C.

wave functions are very close at distances $\leq 4.0$ fm what confirms the mirror symmetry of $(p^{12}\mathrm{C})_{2s^+_{1/2}}$ and $(n^{12}\mathrm{C})_{2s^+_{1/2}}$ systems.

In Fig. 2 are shown the $\frac{\Gamma_{p\,^{12}\mathrm{C}}}{(C_{n\,^{12}\mathrm{C}})^2}$ ratios, which are calculated using Eqs (72) and (75). These calculated ratios are compared with the experimental one. We see that the calculations exceed the experimental value. The $\frac{\Gamma_{p\,^{12}\mathrm{C}}}{(C_{n\,^{12}\mathrm{C}})^2}$ ratio calculated using the simplified Eq. (75) shows the $R_{ch}$ dependence and is equal to $10.13 \times 10^{-5}$ at the peak at $R_{ch} = 5.22$ fm.

Equation (72) provides the $\frac{\Gamma_{p\,^{12}\mathrm{C}}}{(C_{n\,^{12}\mathrm{C}})^2}$ ratio in terms of the ratio of the Wronskians. Each Wronskian contains the two-body wave function and its radial derivative of the system $(N\,^{12}\mathrm{C})_{2s^+_{1/2}}$, $N = p, n$. Each two-body wave function has one node at $r \approx 2.13$ fm and a minimum at $r \approx 4.0$ fm. . Hence, at some point $r$ the Wronskian in the denominator of Eq. (72) vanishes causing a discontinuity in the ratio $\frac{\Gamma_{p\,^{12}\mathrm{C}}}{(C_{n\,^{12}\mathrm{C}})^2}$. I assume that in the nuclear interior the mirror two-body wave functions are correct (as it should be for the mirror microscopic overlap functions) and calculate the ratio at $E_{ch} \geq 4$ fm. At $r = 4$ fm $\frac{\Gamma_{p\,^{12}\mathrm{C}}}{(C_{n\,^{12}\mathrm{C}})^2} = 8.1 \times 10^{-5}$ while the correct value of this ratio obtained at large $R_{ch}$ is $9.8 \times 10^{-5}$, which is close to the peak value of the ratio obtained using Eq. (75).

Both used equations provide the values of the $\frac{\Gamma_{p\,^{12}\mathrm{C}}}{(C_{n\,^{12}\mathrm{C}})^2}$ ratio, which exceed the experimental one. It means that more accurate internal overlap functions are required and the two-body wave functions used here demonstrate the accuracy of the Wronskian method. However, there is another important conclusion: the simple Eq. (75) in the peak gives the same result as the asymptotic ratio given by Eq. (72).

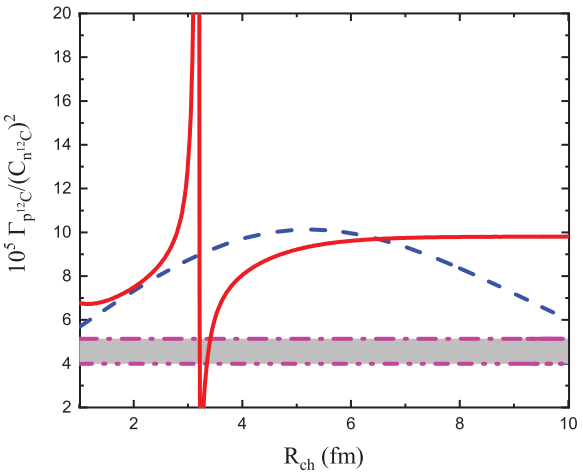


FIG. 2: The grey band is the experimental $\frac{\Gamma_{p\,^{12}\mathrm{C}}}{(C_{n\,^{12}\mathrm{C}})^2}$ ratio of the resonance width of the resonance state $^{13}\mathrm{N}(2s^+_{1/2})$ and the ANC of the mirror bound state $^{13}\mathrm{C}(2s^+_{1/2})$; the red dashed-dotted-dotted line and the red dashed-dotted lines are the low and upper limits of this experimental ratio; the solid red line is the $\frac{\Gamma_{p\,^{12}\mathrm{C}}}{(C_{n\,^{12}\mathrm{C}})^2}$ ratio as a function of $R_{ch}$ calculated using Eq. (72); the blue dotted line is the $\frac{\Gamma_{p\,^{12}\mathrm{C}}}{(C_{n\,^{12}\mathrm{C}})^2}$ ratio calculated as a function of $R_{ch}$ using Eq. (75).

### B. Comparison of resonance width for $^{13}\mathrm{N}(\mathbf{1d_{5/2}}) \to {}^{12}\mathrm{C}(\mathbf{0.0}\,\mathrm{MeV}) + \mathbf{p}$ and mirror ANC for virtual decay $^{13}\mathrm{C}(\mathbf{1d_{5/2}}) \to {}^{12}\mathrm{C}(\mathbf{0.0}\,\mathrm{MeV}) + \mathbf{n}$

As the second example I consider the isobaric analogue states $1d_{5/2}$ in the mirror nuclei $^{13}$N and $^{13}$C. The resonance energy of $^{13}\mathrm{N}(1d_{5/2})$ is $E_{p^{12}\mathrm{C}(0)} = 1.6065$ MeV with the resonance width of $\Gamma_{p\,^{12}\mathrm{C}} = 0.047 \pm 0.0008$ MeV [29]. The neutron binding energy of the mirror state $^{13}\mathrm{C}(1d_{5/2})$ is $\varepsilon_{n^{12}\mathrm{C}} = 1.09635$ MeV with the experimental ANC $C^2_{n^{12}\mathrm{C}} = 0.0225$ fm$^{-1}$ [30]. The experimental ratio is $\Gamma_{p\,^{12}\mathrm{C}}/C^2_{n\,^{12}\mathrm{C}} = (1.1 \pm 0.2) \times 10^{-2}$ .

In Fig. 3 are shown the radial wave functions of the mirror states. Following the $R$-matrix procedure, both wave functions are normalized to unity over the internal volume with the radius $R_{ch} = 3$ fm. We see that the mirror wave functions are very close at distances $r \leq 4$ fm what confirms the mirror symmetry of $(p^{12}\mathrm{C})_{1d^+_{5/2}}$ and $(n^{12}\mathrm{C})_{1d^+_{5/2}}$ systems. In Fig. 4 are shown the $\frac{\Gamma_{p\,^{12}\mathrm{C}}}{(C_{n\,^{12}\mathrm{C}})^2}$ ratios calculated using Eqs (72) and (75), which are compared with the experimental ratio. We see that the calculated ratios are closer to the experimental ratio than in the previous case and both equations give quite reasonable results. The $\frac{\Gamma_{p\,^{12}\mathrm{C}}}{(C_{n\,^{12}\mathrm{C}})^2}$ ratio calculated using the simplified Eq. (75) shows the $R_{ch}$ dependence and is equal to 0.0141 at the peak at $R_{ch} = 3.95$ fm. In the case under consideration the bound-state wave function does not have nodes at $r > 0$. That is why the $\frac{\Gamma_{p\,^{12}\mathrm{C}}}{(C_{n\,^{12}\mathrm{C}})^2}$ ratio calculated using Eq. (72) is a smooth function of $R_{ch}$ . This equation gives $\frac{\Gamma_{p\,^{12}\mathrm{C}}}{(C_{n\,^{12}\mathrm{C}})^2} = 0.0135$ at $R_{ch} = 4$ fm, which differs very little from its correct asymptotic value of 0.0143. Again, as in the previous case, our calculations show that the simple Eq. (75) can give the results close to the Wronskian method.

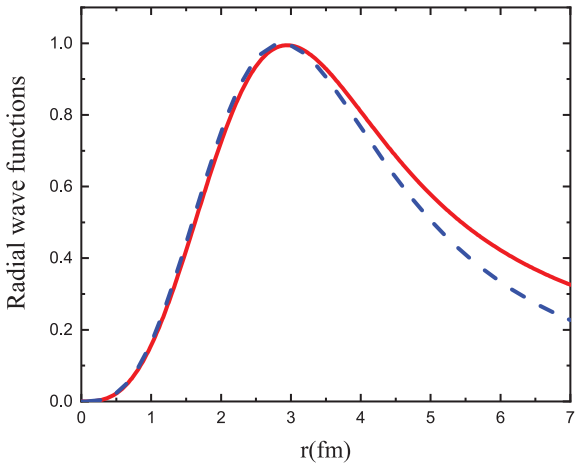


FIG. 3: Solid red line: The radial wave function of the $(p^{12}\mathrm{C})_{1d^+_{5/2}}$ resonance state; dashed blue line: the radial wave function of the mirror $(n^{12}\mathrm{C})_{1d^+_{5/2}}$ bound-state. $r$ is the distance between $N$, where $N = p, n$, and the c.m. of $^{12}$C.

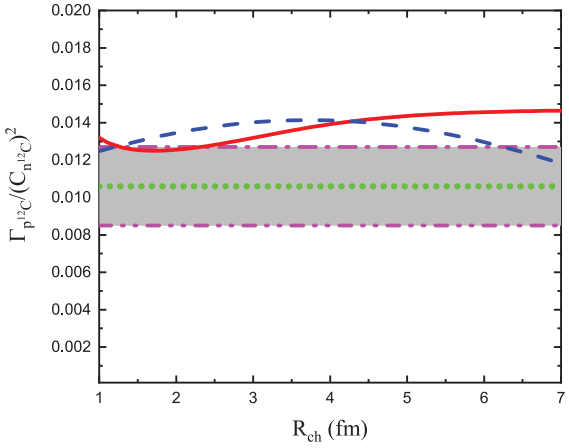


FIG. 4: The grey band is the experimental $\frac{\Gamma_{p\,^{12}\mathrm{C}}}{(C_{n\,^{12}\mathrm{C}})^2}$ ratio of the resonance width of the resonance state $^{13}\mathrm{N}(1d^+_{5/2})$ and the ANC of the mirror bound state $^{13}\mathrm{C}(1d^+_{5/2})$; the red dashed-dotted-dotted line and the red dashed-dotted lines are the low and upper limits of this experimental ratio; the green dotted line is the adopted experimental value of the ratio $\frac{\Gamma_{p\,^{12}\mathrm{C}}}{(C_{n\,^{12}\mathrm{C}})^2} = (1.1\pm0.2)\times10^{-2}$ ; the solid red line is the $\frac{\Gamma_{p\,^{12}\mathrm{C}}}{(C_{n\,^{12}\mathrm{C}})^2}$ ratio as a function of $R_{ch}$ calculated using Eq. (72); the blue dotted line is the $\frac{\Gamma_{p\,^{12}\mathrm{C}}}{(C_{n\,^{12}\mathrm{C}})^2}$ ratio calculated as a function of $R_{ch}$ using Eq. (75).

### C. Comparison of resonance width for $^{15}\mathrm{F}(\mathbf{1d_{5/2}}) \to {}^{14}\mathrm{O}(\mathbf{0.0}\,\mathrm{MeV}) + \mathbf{p}$ and mirror ANC for virtual decay $^{15}\mathrm{C}(\mathbf{1d_{5/2}}) \to {}^{14}\mathrm{C}(\mathbf{0.0}\,\mathrm{MeV}) + \mathbf{n}$

In this section I determine the ratio $\Gamma_{p\,^{14}\mathrm{O}}/C^2_{n\,^{14}\mathrm{C}}$ for the mirror states $^{15}\mathrm{F}(1d_{5/2})$ and $^{15}\mathrm{C}(1d_{5/2})$. The resonance energy and the resonance width of $^{15}\mathrm{F}(1d_{5/2})$ are $E_{p^{14}\mathrm{O}(0)} = 2.77$ MeV and $\Gamma_{p\,^{14}\mathrm{O}} = 0.24 \pm 0.03$ MeV [32]. The binding energy and the ANC of the bound state $^{15}\mathrm{C}(1d_{5/2})$ are $\varepsilon_{n^{14}\mathrm{C}} = 0.478$ MeV and $C^2_{n^{14}\mathrm{C}} = (3.6 \pm 0.8) \times 10^{-3}$ fm$^{-1}$. The experimental ratio $\Gamma_{p\,^{14}\mathrm{O}}/C^2_{n\,^{14}\mathrm{C}} = 0.338 \pm 0.001$ .

This is the most difficult case because the resonance state is not potential. It is clear from Fig. 5.

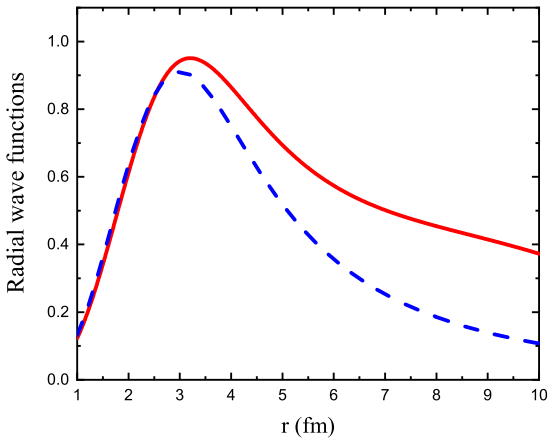


FIG. 5: Solid red line: the radial wave function of the $(p^{14}\mathrm{O})_{1d_{5/2}}$ resonance state; dashed blue line: the radial wave function of the mirror $(n^{14}\mathrm{C})_{1d_{5/2}}$ bound-state. $r$ is the distance between the nucleon and the c.m. of the nucleus.

The mirror wave functions are normalized in the internal region $r \leq 3.2$ fm. They begin to deviate at $r > 3.0$ fm. Because the resonance width in the case under consideration is much wider than in the previous cases, the calculated in the potential model resonant wave function in the external region differs significantly from the tail of the bound-state wave function. That is why the Wronskian ratio does not have an asymptote at large $r$. But the idea of the Wronskian method is to determine the $\Gamma_{p\,^{14}\mathrm{C}}/C^2_{n\,^{14}\mathrm{C}}$ ratio using the mirror wave functions in the internal region where they practically coincide.

In Fig. 6 is shown the $\Gamma_{p\,^{14}\mathrm{O}}/C^2_{n\,^{14}\mathrm{C}}$ ratio calculated using the Wronskian method and the simplified Eq. (75). The Wronskian ratio at 4.0 fm is 0.32 while Eq. (75) gives 0.31. Both values are very close to the experimental ratio.

### D. Comparison of resonance width for $^{18}\mathrm{Ne}(\mathbf{1^-}) \to {}^{14}\mathrm{O}(\mathbf{0.0}\,\mathrm{MeV}) + \alpha$ and mirror ANC for virtual decay $^{18}\mathrm{O}(\mathbf{1^-}) \to {}^{14}\mathrm{C}(\mathbf{0.0}\,\mathrm{MeV}) + \alpha$

In this section I determine the ratio $\Gamma_{\alpha\,^{14}\mathrm{O}}/C^2_{\alpha\,^{14}\mathrm{C}}$ for the mirror states $^{18}\mathrm{Ne}(1^-)$ and $^{18}\mathrm{O}(1^-)$. The resonance energy is $E_{\alpha^{14}\mathrm{O}(0)} = 1.038$ MeV . The binding energy of the bound state $^{18}\mathrm{O}(1^-)$ is $\varepsilon_{\alpha^{14}\mathrm{C}} = 0.027$ MeV. The resonance width and the ANC of the mirror states are unknown.

The purpose of this section is to show that the ratio $\Gamma_{\alpha\,^{14}\mathrm{O}}/C^2_{\alpha\,^{14}\mathrm{C}}$ does not depend on the number of the nodes of the mirror wave functions. The potential model search showed that for the given resonance energy and binding energy for $l = 1$ the mirror wave functions have at $r > 0$ the number of nodes $N = 4$ or 6 . The normalization region of the mirror wave functions is $r \leq 7.2$ fm for $N = 6$ and $r \leq 6.73$ fm for $N = 4$. In Figs 7 and 8 are shown the radial wave functions and the ratio $\Gamma_{\alpha\,^{14}\mathrm{O}}/C^2_{\alpha\,^{14}\mathrm{C}}$ for the number of the nodes $N = 4$ and 6.

One can see that the mirror wave functions practically coincide up to $r = 15$ fm. It means that the simplified Eq. (75) can be used up to 15 fm. The ratio $\Gamma_{\alpha\,^{14}\mathrm{O}}/C^2_{\alpha\,^{14}\mathrm{C}}$ calculated using Eq. (72) is the same for $N = 4$ and 6. Because the mirror wave functions practically identical in the external region the ratio $\Gamma_{\alpha\,^{14}\mathrm{O}}/C^2_{\alpha\,^{14}\mathrm{C}}$ calculated using the Wronskian method (Eq. (72)) has an asymptote. The calculated for $N = 4$, 6 ratio reaches its asymptotic value at $R_{ch} = 7.5$ fm which is $\Gamma_{\alpha\,^{14}\mathrm{O}}/C^2_{\alpha\,^{14}\mathrm{C}} = 3.48 \times 10^{52}$. The maximum of $\Gamma_{\alpha\,^{14}\mathrm{O}}/C^2_{\alpha\,^{14}\mathrm{C}}$ calculated using Eq. (75) at $R_{ch} = 9$ fm is $3.42 \times 10^{52}$. This comparison demonstrates again that in the absence of the microscopic internal

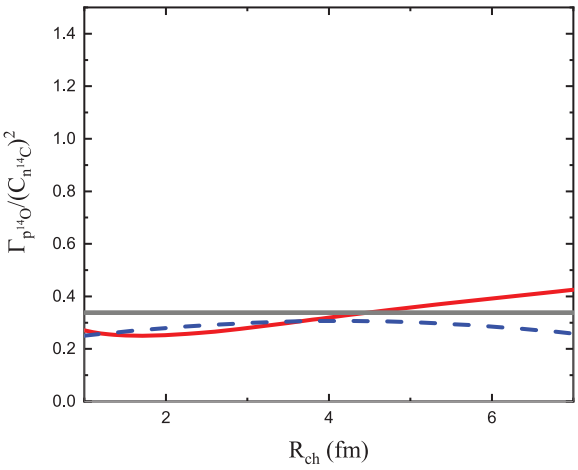


FIG. 6: The grey band is the experimental $\frac{\Gamma_{p\,^{14}\mathrm{O}}}{(C_{n\,^{14}\mathrm{C}})^2}$ ratio for the resonance state $^{15}\mathrm{F}(1d^+_{5/2})$ and the mirror bound state $^{15}\mathrm{C}(1d^+_{5/2})$; the solid red line is the $\frac{\Gamma_{p\,^{14}\mathrm{O}}}{(C_{n\,^{14}\mathrm{C}})^2}$ ratio as a function of $R_{ch}$ calculated using Eq. (72); the blue dashed line is the $\frac{\Gamma_{p\,^{14}\mathrm{O}}}{(C_{n\,^{14}\mathrm{C}})^2}$ ratio calculated as a function of $R_{ch}$ using Eq. (75).

overlap functions both the Wronskian and the simplified method given by Eq. (75) can be used and give very close results.

### E. Comparison of resonance width for $^{17}\mathrm{F}(\mathbf{s_{1/2}}) \to {}^{13}\mathrm{N}(\mathbf{0.0}\,\mathrm{MeV}) + \alpha$ and mirror ANC for virtual decay $^{17}\mathrm{O}(\mathbf{s_{1/2}}) \to {}^{13}\mathrm{C}(\mathbf{0.0}\,\mathrm{MeV}) + \alpha$

The last case, which I consider, is the determination of the ratio $\frac{\Gamma_{\alpha\,^{13}\mathrm{N}}}{(C_{\alpha\,^{13}\mathrm{C}})^2}$ of the resonance state $^{17}\mathrm{F}(1/2^+)$ and the mirror bound state $^{17}\mathrm{O}(1/2^+)$. The orbital momentum of the mirror states is $l = 1$ and the resonance energy is $E_{\alpha\,^{13}\mathrm{N}(0)} = 0.7371$ MeV [32]. The location of the state $^{17}\mathrm{O}(1/2^+)$ is questionable. The excitation energy $E_x$ of the state $^{17}\mathrm{O}(1/2^+)$ is $6356 \pm 8$ keV [32]. Taking into account that the $\alpha - {}^{13}\mathrm{C}$ threshold is located at 6359.2 keV one finds that this $1/2^+$ level is the located at $E_{\alpha^{13}\mathrm{C}} = -3 \pm 8$ keV, that is, it can be a subthreshold bound state or a resonance [32]. This location of the level $^{17}\mathrm{O}(1/2^+)$ was adopted in the previous analyses of the direct measurements including the latest one in [33]. If this level is the subthreshold bound state, then its reduced width is related to the ANC of this level. However, in a recent paper [34] it has been determined that this level is actually a resonance located at $E_{\alpha^{13}\mathrm{C}} = 4.7 \pm 3$ keV. Because the possible subthreshold state and near threshold resonance are located very close to each other the reduced widths corresponding to these two levels are very close. Here in the analysis I still assume that $^{17}\mathrm{O}(1/2^+)$ is the bound state with the binding energy of $-3$ keV. I adopt the ANC of this subthreshold state $C^2_{\alpha^{13}\mathrm{C}} = 4.4 \times 10^{169}$ fm$^{-1}$ [35].

The calculated mirror resonance and bound state wave functions are shown in Fig. 9. They are normalized in the internal region $r \leq 5.2$ fm. Both wave functions practically identical up to $R_{ch} \leq 15$ fm.

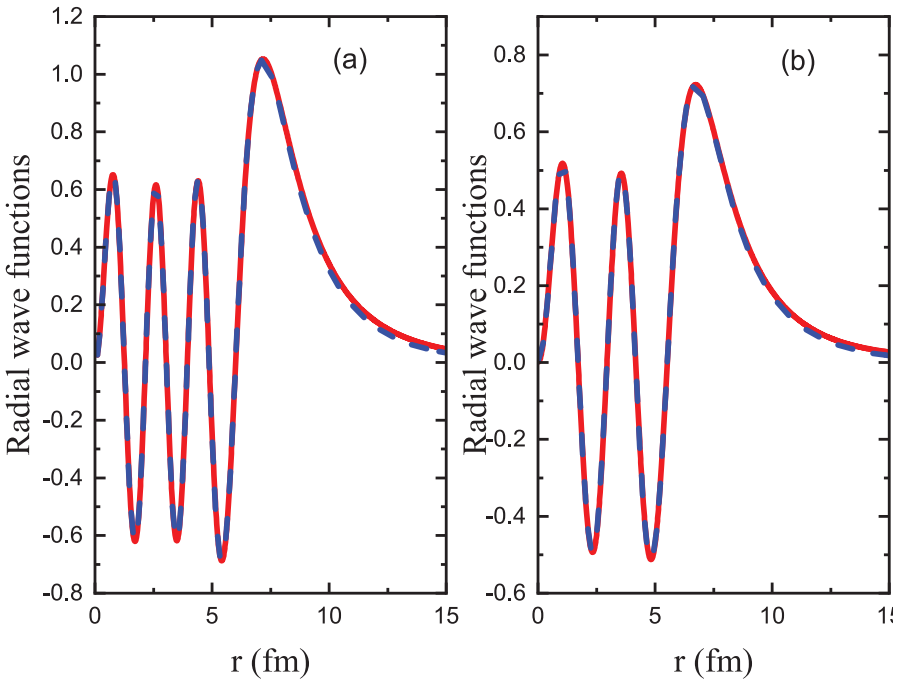


FIG. 7: Panel (a): the mirror radial wave functions for $N = 6$; the solid red line is the $(\alpha^{14}\mathrm{O})_{1^-}$ resonance wave function; the dashed blue line is the radial wave function of the mirror $(\alpha^{14}\mathrm{C})_{1^-}$ bound-state. $r$ is the distance between the $\alpha$-particle and the c.m. of the nucleus. Panel (b): notations are the same as in panel (a) but for $N = 4$.

In Fig. 10 the $\frac{\Gamma_{\alpha\,^{13}\mathrm{N}}}{(C_{\alpha\,^{13}\mathrm{C}})^2}$ ratio is calculated using the Wronskian Eq. (72) and the simple Eq. (75). The asymptotic value of the ratio is $\frac{\Gamma_{\alpha\,^{13}\mathrm{N}}}{(C_{\alpha\,^{13}\mathrm{C}})^2} = 4.48 \times 10^{-178}$. The value of the $\frac{\Gamma_{\alpha\,^{13}\mathrm{N}}}{(C_{\alpha\,^{13}\mathrm{C}})^2}$ at the border of the internal region $R_{ch} = 5.2$ fm is very close to its asymptotic value. Eq. (75) gives $\frac{\Gamma_{\alpha\,^{13}\mathrm{N}}}{(C_{\alpha\,^{13}\mathrm{C}})^2} = 4.55 \times 10^{-178}$. Taking into account the adopted value of the ANC $C_{\alpha\,^{13}\mathrm{C}}$ and the experimental ratio $\frac{\Gamma_{\alpha\,^{13}\mathrm{N}}}{(C_{\alpha\,^{13}\mathrm{C}})^2} = 4.48 \times 10^{-178}$ one obtains from the Wronskian ratio the resonance width $\Gamma_{\alpha\,^{13}N} = 4.48 \times 10^{-178} \times 4.4 \times 10^{169} \times \hbar c = 3.9$ eV.

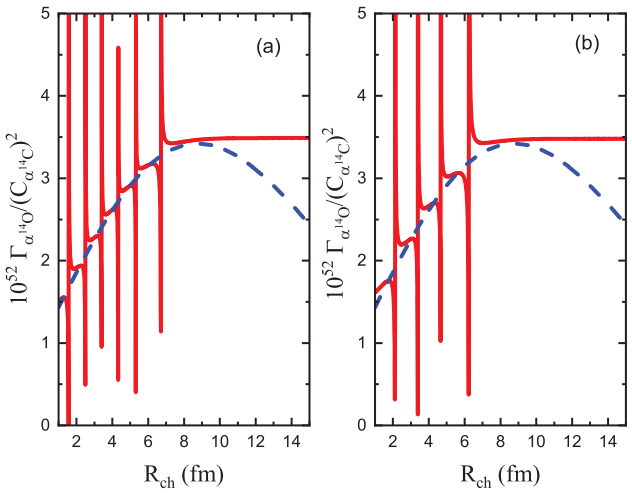


FIG. 8: Panel (a): the $\frac{\Gamma_{\alpha\,^{14}\mathrm{O}}}{(C_{\alpha\,^{14}\mathrm{C}})^2}$ ratio for the resonance state $^{18}\mathrm{Ne}(1^-)$ and the mirror bound state $^{18}\mathrm{O}(1^-)$ for $N=6$; the solid red line is the $\frac{\Gamma_{\alpha\,^{14}\mathrm{O}}}{(C_{\alpha\,^{14}\mathrm{C}})^2}$ ratio as a function of $R_{ch}$ calculated using Eq. (72); the blue dashed line is the $\frac{\Gamma_{\alpha\,^{14}\mathrm{O}}}{(C_{\alpha\,^{14}\mathrm{C}})^2}$ ratio calculated as a function of $R_{ch}$ using Eq. (75). Panel (b): notations are the same as in panel (a) but for $N=4$.

## VIII. APPENDIX

In this Appendix is shown that Zeldovich regularization procedure can be used for normalization of the resonance wave function $u_{k_p l_B}(r)$ both for exponentially decaying potentials and potentials with the Coulomb tail. The normalization of the resonance wave function depends on its tail. Taking into account Eq. (13) it is enough to consider the integral

$$I(\beta,\nu,z)=\int\limits_0^\infty \mathrm{d}r\, e^{-\beta\, r^2}\, e^{z\, r}\, r^\nu. \tag{76}$$

Here, $z=2\,i\,k_{aA(\mathcal{R})}\,r=2\,i\,k_{aA(0)}\,r+2\,\mathrm{Im}k_{aA(\mathcal{R})}\,r$. It is assumed that $k_{aA(0)}>\mathrm{Im}k_{aA(\mathcal{R})}$, as it should be for physical resonances. Then $\mathrm{Re}z^2<0$. Also

$$\nu=-2\,i\,\eta_{aA}^{(\mathcal{R})}=-2i\,\frac{\gamma}{k_{aA(0)}-i\,\mathrm{Im}\,k_{aA(\mathcal{R})}}=-2\,i\,\frac{\gamma\,k_{aA(0)}}{k_{aA(0)}^2+(\mathrm{Im}k_{aA(\mathcal{R})})^2}+2\,\frac{\gamma\,\mathrm{Im}k_{aA(\mathcal{R})}}{k_{aA(0)}^2+(\mathrm{Im}k_{aA(\mathcal{R})})^2}, \tag{77}$$

$\gamma=Z_a\,Z_A\,\mu_{aA}/137$. Thus, one can see that for the repulsive Coulomb potential $\mathrm{Re}\nu>0$ using Eq. (3.462.1) from [36] one gets

$$I(\beta,\nu,z)=\Gamma(\nu+1)\,(2\,\beta)^{-(\nu+1)/2}\,e^{z^2/(8\,\beta)}\,D_{-\nu-1}(-z/\sqrt{2\,\beta}). \tag{78}$$

Here $D_\sigma(x)$ is the parabolic cylinder function. For $\mathrm{Re}z^2<0$ using Eq. (9.246.1) from [36] one gets

$$I(0,\,\nu,\,z)=\lim_{\beta\to+0}I(\beta,\,\nu,\,z)=\Gamma(\nu+1)\,(-z)^{-\nu-1}. \tag{79}$$

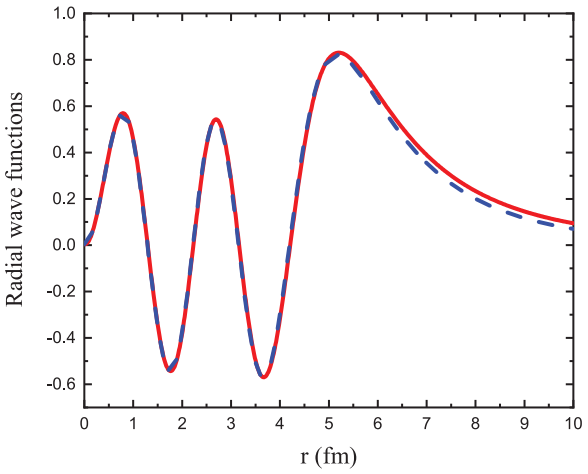


FIG. 9: The solid red line is the $(\alpha^{13}\mathrm{N})_{1/2^+}$ resonance wave function; the dashed blue line is the radial wave function of the mirror $(\alpha^{13}\mathrm{C})_{1/2^+}$ bound-state. $r$ is the distance between the $\alpha$-particle and the c.m. of the nucleus.

Thus the regularization procedure used by Zeldovich is applicable and for the physical resonances $k_{aA(0)} > \mathrm{Im}k_{aA(\mathcal{R})}$ the integral in Eq. (76) does exist and converges in the lim $\beta \to +0$ .

Let me consider now the integral

$$I_R(\beta,\nu,z) = \int_R^\infty \mathrm{d}r\, e^{-\beta\, r^2}\, e^{z\, r}\, r^\nu. \tag{80}$$

Integrating it by parts one gets

$$\lim_{\beta\to+0} I_R(\beta,\nu,z) = -\frac{R^\nu}{z}\, e^{z\, R}\left[1 - \frac{\nu}{z\, R} + O(\frac{1}{z^2\, R^2})\right]. \tag{81}$$

## IX. ACKNOWLEDGMENTS

This work was supported by the U.S. DOE Grant No. DE-FG02-93ER40773, NNSA Grant No. DE-NA0003841 and U.S. NSF Award No. PHY-1415656.

[1] L. D. Blokhintsev, I. Borbely, and E. I. Dolinskii, Fiz. Elem. Chastits t. Yadra **8**, 1189 (1977) [Sov. J. Part. Nucl. **8**, 485 (1977)].

[2] L. D. Blokhintsev, A. M. Mukhamedzhanov, A. N. Safronov, Fiz. Elem. Chastits t. Yadra **15**, 1296 (1984) [Sov. J. Part. Nucl. **15**, 580 (1984)].

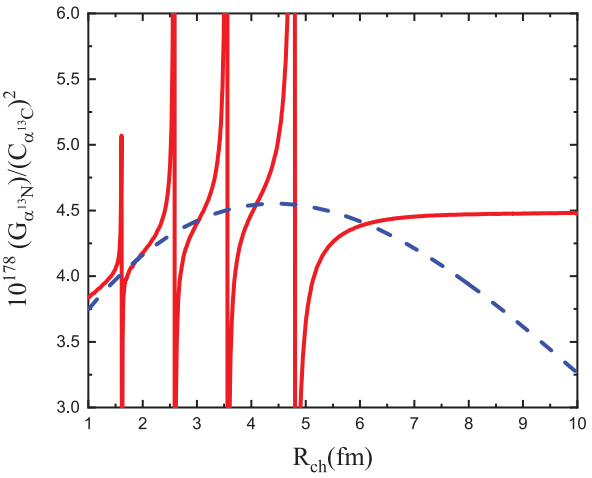


FIG. 10: The $\frac{\Gamma_{\alpha\,^{13}\mathrm{N}}}{(C_{\alpha\,^{13}\mathrm{C}})^2}$ ratio for the resonance state $^{17}$F$(1/2^+)$ and the mirror bound state $^{17}$O$(1/2^+)$; the solid red line is the $\frac{\Gamma_{\alpha\,^{13}\mathrm{N}}}{(C_{\alpha\,^{13}\mathrm{C}})^2}$ ratio as a function of $R_{ch}$ calculated using Eq. (72); the blue dashed line is the $\frac{\Gamma_{\alpha\,^{13}\mathrm{N}}}{(C_{\alpha\,^{13}\mathrm{C}})^2}$ ratio calculated as a function of $R_{ch}$ using Eq. (75).


[3] A. M. Mukhamedzhanov and N. K. Timofeyuk, Pis'ma Eksp. Teor. Fiz. **51**, 247 (1990) [JETP Lett. **51**, 282 (1990)].
[4] A. M. Mukhamedzhanov, C. A. Gagliardi, and R. E. Tribble, Phys. Rev. **C 63**, 024612 (2001) .
[5] A. M. Mukhamedzhanov, L. D. Blokhintsev, and B. F. Irgaziev, Phys. Rev. **C 83**, 055805 (2011).
[6] A. M. Mukhamedzhanov and N. K. Timofeyuk, Sov. J. Nucl. Phys. 51, 431 (1990) [Yad. Fiz. 51, 679 (1990)].
[7] Xiaodong Tang, A. Azhari, C. A. Gagliardi, A. M. Mukhamedzhanov, F. Pirlepesov, L. Trache, R. E. Tribble, V. Burjan, V. Kroha, and F. Carstoiu, Phys. Rev. **C 67**, 015804 (2003).
[8] A. M. Mukhamedzhanov, M. La Cognata and V. Kroha, Phys. Rev. **C 83**, 044604 (2011).
[9] A. M. Mukhamedzhanov and R. E. Tribble, Phys. Rev. **C 59**, 3418 (1999).
[10] N. K. Timofeyuk, R. C. Johnson, and A. M. Mukhamedzhanov, Phys. Rev. Lett. **91**, 232501 (2003).
[11] A. M. Mukhamedzhanov, Phys. Rev. **C 86**, 044615 (2012).
[12] R. F. Casten, Nucler Structure from a simple Perrspective, Oxford University Press, New York, 2005.
[13] H. . Kramers, Hand und Jahrbuch der Chemischer Physik **1**, 312 (1938).
[14] W. Heisenberg, Zs f. Naturforsch. **1**, 608 (1946).
[15] C. Möller, Dan. Vid Selsk. Mat. Fys. Medd. **22**, N.19 (1946).
[16] N. Hu, Phys. Rev. **74**, 131 (1948).
[17] Ya. B. Zel'dovich, ZhetF **51**, 1492 (1965).
[18] M. Perelomov, V.S. Popov, M. V. Terentev, ZhETF **51**, 309 (1966).
[19] A. M. Lane and R. G. Thomas, Rev. Mod. Phys. **30**, 257 (1958).
[20] W. T. Pinkston and G. R. Satchler, Nucl. Phys. **72**, 641 (1965)
[21] R. J. Philpott, W. T. Pinkston, and G. R. Satchler, Nucl. Phys. **A119**, 241 (1968).
[22] N.K. Timofeyuk, Nucl. Phys. **A632**, 19 (1998).
[23] R. G. Newton, Scattering Theory of Waves and Particles, 2nd ed., Springer-Verlag, Heidelberg, 1982.
[24] P. Navratil, J. P. Vary and B. R. Barrett, Phys. Rev. **C 62**, 054311 (2000).
[25] P. Navratil, W. E. Ormand, Phys. Rev. **C 68**, 034305 (2003).
[26] S. Quaglioni, P. Navratil, Phys. Rev. Lett. **101**, 092501 (2008).

[27] O. Jensen, G. Hagen, M. Hjorth-Jensen, B. A. Brown, A. Gade, Phys. Rev. Lett. 107, 032501 (2011).
[28] N. K. Timofeyuk, Phys. Rev. **C 84**, 054313 (2011).
[29] F. Ajzenberg-Selove, Nucl. Phys. **A523**, 1 (1991).
[30] Z. H. Liu *et al.*, Phys. Rev. **C 64**, 034312 (2001).
[31] N. Imai *et al.*, Nucl. Phys. **A688**, 281c (2001).
[32] D. R. Tilley, H. R. Weller, and C. M. Cheves, Nucl. Phys. **A564**, 1 (1993).
[33] M. Heil, R. Detwiler, and R. E. Azuma *et al.*, Phys. Rev. **C 78**, 025803 (2008).
[34] T. Faestermann, P. Mohr, R. Hertenberger, and H.-F. Wirth, Phys. Rev. **C 92**, 052802(R) (2015).
[35] A. M. Mukhamedzhanov, Shubhchintak, and C. A. Bertulani, Phys. Rev. **C 96**, 024623 (2017) .
[36] I. S. Gradshteyn and L/ M. Ryzhik, Tables of Integrals, Series and Products, Academic Press, New York, London, 1980.